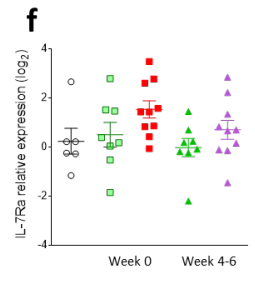
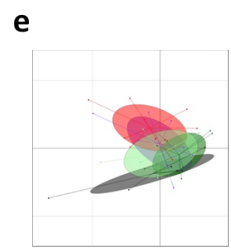
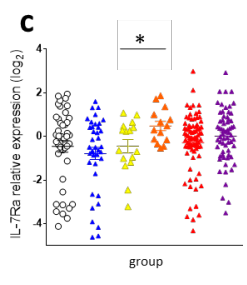
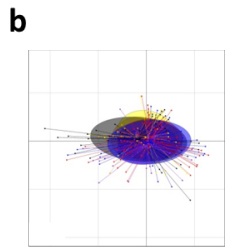
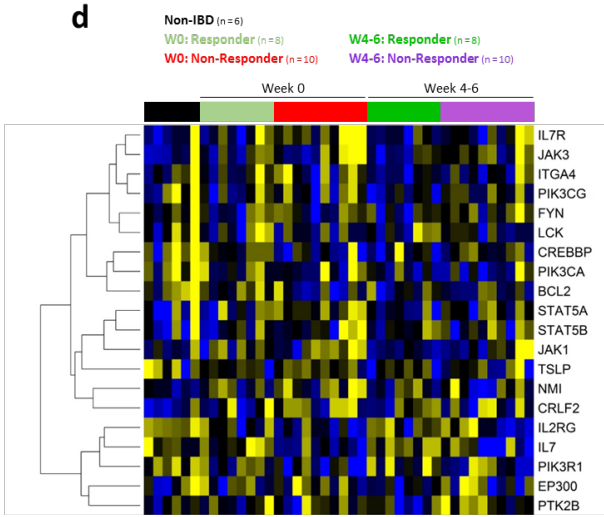
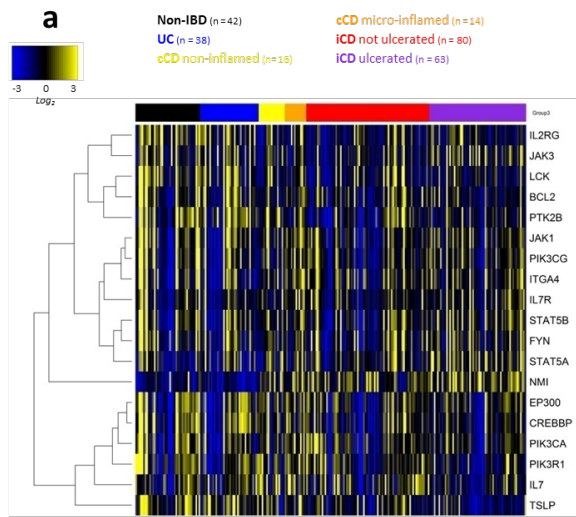


Supplemental data of “*IL-7 receptor influences anti-TNF responsiveness and T cell gut-homing in inflammatory bowel disease*” by Belarif L et al.

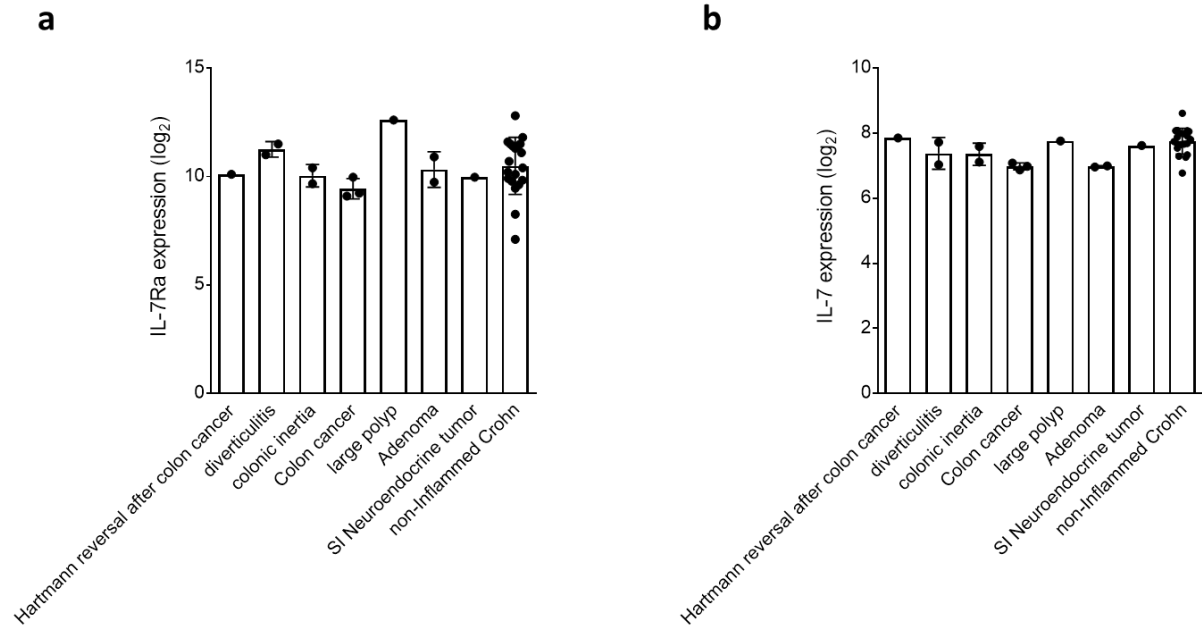
Supplementary Figure 1: *IL7R* and *IL7R* signaling pathway expression in ileal biopsies is not associated with active disease or response to anti-TNF in CD patients.

(a) Heatmap of the expression of the 20 selected genes previously reported as key members of the *IL7R* signaling pathway (39), in ileal biopsies from healthy pediatric controls (black: n = 42) and patients with newly diagnosed and untreated ileal CD (purple: ulcerated n = 63, red: not ulcerated n = 80), colonic CD (yellow: non-inflamed n = 16, orange: micro-inflamed n = 14) or UC (blue: n = 38) (dataset GSE57945) (43). The heatmap represents median centered and colorized expression values in which yellow values indicate over-expression and blue values indicate under-expression. (b) PCA based on expression of the *IL7R* signaling signature in the same group of patients as in (a). (c) Relative *IL7R* expression in the same group of patients as in (a), log₂ FPKM data are normalized to the control median. (d) Heatmap of the *IL7R* signaling signature expression in ileal biopsies from non-IBD controls (black: n = 6) and responder (green: n = 8) or non-responder (red/purple: n = 10) CD patients to anti-TNF therapy (dataset GSE16879) (45). Samples were analyzed within a week before anti-TNF infusion and 4-6 weeks after treatment. (b) PCA of the *IL7R* signaling signature (20 selected genes) in the same group of patients as in (d). (c) Relative *IL7R* expression in the same group of patients as in (d), log₂ data are normalized to the control median. * p<0.05 between indicated groups.



Supplementary Figure 2: *IL7R* and *IL7* expression in different non-IBD controls conditions.

(a) *IL7R* and (b) *IL7* expression in colon biopsies of indicated non-IBD control conditions as compared to non-inflamed mucosa of Crohn's patients (dataset GSE66207) (S1).

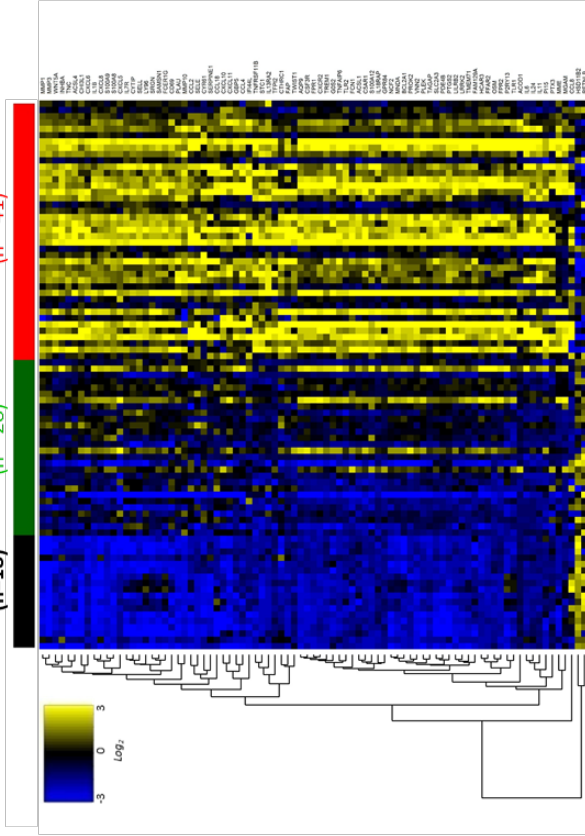


Supplementary Figure 3: Differential gene expression analysis between colon mucosa of responders and non-responders UC patients before therapy with anti-TNF.

(a) Heatmap of the expression of the 85 genes identified with an adjusted p-value < 0.05 and a Log_2 Fold Change (FC) > 1 in colon biopsies of non-IBD controls (n=18), responders (green, n=28) and non-responders (red, n=41) before anti-TNF therapy. Meta-analysis of 3 UC cohorts with histological healing as the anti-TNF response criteria: dataset GSE16879 (43) and GSE12251 (44), and GSE73661 (46). (b) Gene name, Log_2FC and adjusted p-value for each 85 genes as in (a). (c) Gene network for the 85 genes as in (a).

Supplementary figure 3

a Non-IBD (n=18) **WO: Responder** (n = 28) **WO: Non-Responder** (n = 41)



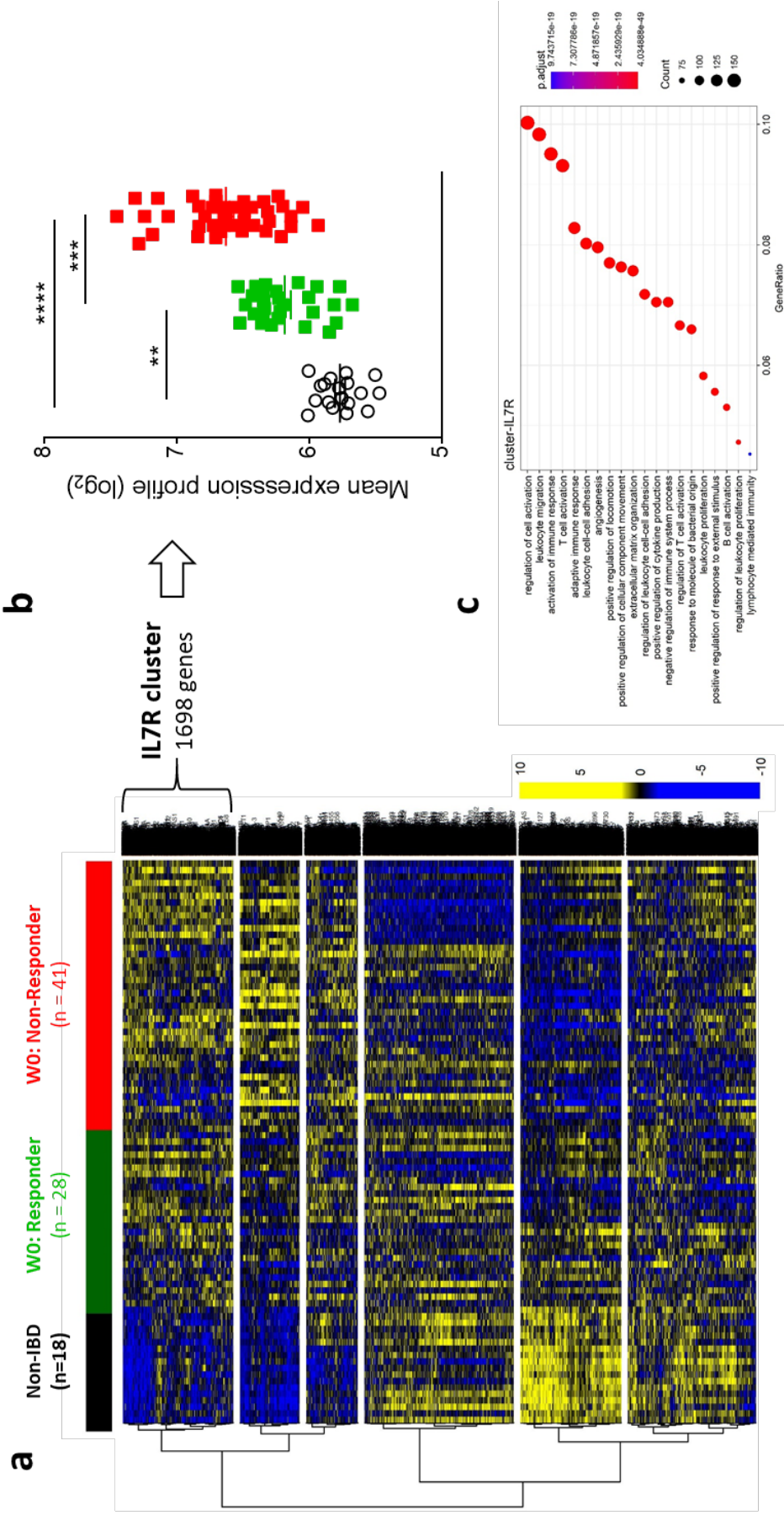
b

Gene Symbol	UniProt ID	Gene Name	Symbol	Log2 C	adjusted p-value
IL13RA2	3598	interleukin 13 receptor subunit alpha 2	IL13RA2	1.67	3.4E-07
TNFRSF1B	4982	TNF receptor superfamily member 1b	TNFRSF1B	2.02	3.4E-07
SFC1	6781	sarcosin 1	SFC1	1.53	2.9E-06
MYO10	1573	myosin X	MYO10	1.53	2.9E-06
ACE3L4	2182	angiotensin-converting enzyme 3-like 4	ACE3L4	1.06	5.4E-06
PTGS2	5743	prostaglandin-endoperoxidase synthase 2	PTGS2	2.24	8.8E-06
SRGN	5552	serpin G1	SRGN	1.07	9.0E-06
IL11	3589	interleukin 11	IL11	1.31	1.82E-05
INHBA	3024	inhibin beta A subunit	INHBA	1.52	1.94E-05
IL6	3509	interleukin 6	IL6	2.20	2.47E-05
IL13	3508	interleukin 13	IL13	1.85	2.74E-05
SOX1	6441	sox1	SOX1	1.85	2.74E-05
IL18R2	10288	leukocyte immunoglobulin like receptor B2	IL18R2	1.10	3.11E-05
TLR1	7096	tol like receptor 1	TLR1	1.21	3.18E-05
LY86	23643	lymphocyte antigen 86	LY86	1.18	3.43E-05
GOS2	50486	GOS2	GOS2	1.57	3.7E-05
MMP3	4314	matrix metalloproteinase 3	MMP3	1.73	5.23E-05
CDK1	632	cyclin dependent kinase 1	CDK1	1.75	5.57E-05
CDK2	633	cyclin dependent kinase 2	CDK2	1.75	5.57E-05
CDK4	634	cyclin dependent kinase 4	CDK4	1.75	5.57E-05
CDK6	635	cyclin dependent kinase 6	CDK6	1.75	5.57E-05
CDK8	636	cyclin dependent kinase 8	CDK8	1.75	5.57E-05
CDK9	637	cyclin dependent kinase 9	CDK9	1.75	5.57E-05
CDK10	638	cyclin dependent kinase 10	CDK10	1.75	5.57E-05
CDK11	639	cyclin dependent kinase 11	CDK11	1.75	5.57E-05
CDK12	640	cyclin dependent kinase 12	CDK12	1.75	5.57E-05
CDK13	641	cyclin dependent kinase 13	CDK13	1.75	5.57E-05
CDK14	642	cyclin dependent kinase 14	CDK14	1.75	5.57E-05
CDK15	643	cyclin dependent kinase 15	CDK15	1.75	5.57E-05
CDK16	644	cyclin dependent kinase 16	CDK16	1.75	5.57E-05
CDK17	645	cyclin dependent kinase 17	CDK17	1.75	5.57E-05
CDK18	646	cyclin dependent kinase 18	CDK18	1.75	5.57E-05
CDK19	647	cyclin dependent kinase 19	CDK19	1.75	5.57E-05
CDK20	648	cyclin dependent kinase 20	CDK20	1.75	5.57E-05
CDK21	649	cyclin dependent kinase 21	CDK21	1.75	5.57E-05
CDK22	650	cyclin dependent kinase 22	CDK22	1.75	5.57E-05
CDK23	651	cyclin dependent kinase 23	CDK23	1.75	5.57E-05
CDK24	652	cyclin dependent kinase 24	CDK24	1.75	5.57E-05
CDK25	653	cyclin dependent kinase 25	CDK25	1.75	5.57E-05
CDK26	654	cyclin dependent kinase 26	CDK26	1.75	5.57E-05
CDK27	655	cyclin dependent kinase 27	CDK27	1.75	5.57E-05
CDK28	656	cyclin dependent kinase 28	CDK28	1.75	5.57E-05
CDK29	657	cyclin dependent kinase 29	CDK29	1.75	5.57E-05
CDK30	658	cyclin dependent kinase 30	CDK30	1.75	5.57E-05
CDK31	659	cyclin dependent kinase 31	CDK31	1.75	5.57E-05
CDK32	660	cyclin dependent kinase 32	CDK32	1.75	5.57E-05
CDK33	661	cyclin dependent kinase 33	CDK33	1.75	5.57E-05
CDK34	662	cyclin dependent kinase 34	CDK34	1.75	5.57E-05
CDK35	663	cyclin dependent kinase 35	CDK35	1.75	5.57E-05
CDK36	664	cyclin dependent kinase 36	CDK36	1.75	5.57E-05
CDK37	665	cyclin dependent kinase 37	CDK37	1.75	5.57E-05
CDK38	666	cyclin dependent kinase 38	CDK38	1.75	5.57E-05
CDK39	667	cyclin dependent kinase 39	CDK39	1.75	5.57E-05
CDK40	668	cyclin dependent kinase 40	CDK40	1.75	5.57E-05
CDK41	669	cyclin dependent kinase 41	CDK41	1.75	5.57E-05
CDK42	670	cyclin dependent kinase 42	CDK42	1.75	5.57E-05
CDK43	671	cyclin dependent kinase 43	CDK43	1.75	5.57E-05
CDK44	672	cyclin dependent kinase 44	CDK44	1.75	5.57E-05
CDK45	673	cyclin dependent kinase 45	CDK45	1.75	5.57E-05
CDK46	674	cyclin dependent kinase 46	CDK46	1.75	5.57E-05
CDK47	675	cyclin dependent kinase 47	CDK47	1.75	5.57E-05
CDK48	676	cyclin dependent kinase 48	CDK48	1.75	5.57E-05
CDK49	677	cyclin dependent kinase 49	CDK49	1.75	5.57E-05
CDK50	678	cyclin dependent kinase 50	CDK50	1.75	5.57E-05
CDK51	679	cyclin dependent kinase 51	CDK51	1.75	5.57E-05
CDK52	680	cyclin dependent kinase 52	CDK52	1.75	5.57E-05
CDK53	681	cyclin dependent kinase 53	CDK53	1.75	5.57E-05
CDK54	682	cyclin dependent kinase 54	CDK54	1.75	5.57E-05
CDK55	683	cyclin dependent kinase 55	CDK55	1.75	5.57E-05
CDK56	684	cyclin dependent kinase 56	CDK56	1.75	5.57E-05
CDK57	685	cyclin dependent kinase 57	CDK57	1.75	5.57E-05
CDK58	686	cyclin dependent kinase 58	CDK58	1.75	5.57E-05
CDK59	687	cyclin dependent kinase 59	CDK59	1.75	5.57E-05
CDK60	688	cyclin dependent kinase 60	CDK60	1.75	5.57E-05
CDK61	689	cyclin dependent kinase 61	CDK61	1.75	5.57E-05
CDK62	690	cyclin dependent kinase 62	CDK62	1.75	5.57E-05
CDK63	691	cyclin dependent kinase 63	CDK63	1.75	5.57E-05
CDK64	692	cyclin dependent kinase 64	CDK64	1.75	5.57E-05
CDK65	693	cyclin dependent kinase 65	CDK65	1.75	5.57E-05
CDK66	694	cyclin dependent kinase 66	CDK66	1.75	5.57E-05
CDK67	695	cyclin dependent kinase 67	CDK67	1.75	5.57E-05
CDK68	696	cyclin dependent kinase 68	CDK68	1.75	5.57E-05
CDK69	697	cyclin dependent kinase 69	CDK69	1.75	5.57E-05
CDK70	698	cyclin dependent kinase 70	CDK70	1.75	5.57E-05
CDK71	699	cyclin dependent kinase 71	CDK71	1.75	5.57E-05
CDK72	700	cyclin dependent kinase 72	CDK72	1.75	5.57E-05
CDK73	701	cyclin dependent kinase 73	CDK73	1.75	5.57E-05
CDK74	702	cyclin dependent kinase 74	CDK74	1.75	5.57E-05
CDK75	703	cyclin dependent kinase 75	CDK75	1.75	5.57E-05
CDK76	704	cyclin dependent kinase 76	CDK76	1.75	5.57E-05
CDK77	705	cyclin dependent kinase 77	CDK77	1.75	5.57E-05
CDK78	706	cyclin dependent kinase 78	CDK78	1.75	5.57E-05
CDK79	707	cyclin dependent kinase 79	CDK79	1.75	5.57E-05
CDK80	708	cyclin dependent kinase 80	CDK80	1.75	5.57E-05
CDK81	709	cyclin dependent kinase 81	CDK81	1.75	5.57E-05
CDK82	710	cyclin dependent kinase 82	CDK82	1.75	5.57E-05
CDK83	711	cyclin dependent kinase 83	CDK83	1.75	5.57E-05
CDK84	712	cyclin dependent kinase 84	CDK84	1.75	5.57E-05
CDK85	713	cyclin dependent kinase 85	CDK85	1.75	5.57E-05
CDK86	714	cyclin dependent kinase 86	CDK86	1.75	5.57E-05
CDK87	715	cyclin dependent kinase 87	CDK87	1.75	5.57E-05
CDK88	716	cyclin dependent kinase 88	CDK88	1.75	5.57E-05
CDK89	717	cyclin dependent kinase 89	CDK89	1.75	5.57E-05
CDK90	718	cyclin dependent kinase 90	CDK90	1.75	5.57E-05
CDK91	719	cyclin dependent kinase 91	CDK91	1.75	5.57E-05
CDK92	720	cyclin dependent kinase 92	CDK92	1.75	5.57E-05
CDK93	721	cyclin dependent kinase 93	CDK93	1.75	5.57E-05
CDK94	722	cyclin dependent kinase 94	CDK94	1.75	5.57E-05
CDK95	723	cyclin dependent kinase 95	CDK95	1.75	5.57E-05
CDK96	724	cyclin dependent kinase 96	CDK96	1.75	5.57E-05
CDK97	725	cyclin dependent kinase 97	CDK97	1.75	5.57E-05
CDK98	726	cyclin dependent kinase 98	CDK98	1.75	5.57E-05
CDK99	727	cyclin dependent kinase 99	CDK99	1.75	5.57E-05
CDK100	728	cyclin dependent kinase 100	CDK100	1.75	5.57E-05
CDK101	729	cyclin dependent kinase 101	CDK101	1.75	5.57E-05
CDK102	730	cyclin dependent kinase 102	CDK102	1.75	5.57E-05
CDK103	731	cyclin dependent kinase 103	CDK103	1.75	5.57E-05
CDK104	732	cyclin dependent kinase 104	CDK104	1.75	5.57E-05
CDK105	733	cyclin dependent kinase 105	CDK105	1.75	5.57E-05
CDK106	734	cyclin dependent kinase 106	CDK106	1.75	5.57E-05
CDK107	735	cyclin dependent kinase 107	CDK107	1.75	5.57E-05
CDK108	736	cyclin dependent kinase 108	CDK108	1.75	5.57E-05
CDK109	737	cyclin dependent kinase 109	CDK109	1.75	5.57E-05
CDK110	738	cyclin dependent kinase 110	CDK110	1.75	5.57E-05
CDK111	739	cyclin dependent kinase 111	CDK111	1.75	5.57E-05
CDK112	740	cyclin dependent kinase 112	CDK112	1.75	5.57E-05
CDK113	741	cyclin dependent kinase 113	CDK113	1.75	5.57E-05
CDK114	742	cyclin dependent kinase 114	CDK114	1.75	5.57E-05
CDK115	743	cyclin dependent kinase 115	CDK115	1.75	5.57E-05
CDK116	744	cyclin dependent kinase 116	CDK116	1.75	5.57E-05
CDK117	745	cyclin dependent kinase 117	CDK117	1.75	5.57E-05
CDK118	746	cyclin dependent kinase 118	CDK118	1.75	5.57E-05
CDK119	747	cyclin dependent kinase 119	CDK119	1.75	5.57E-05
CDK120	748	cyclin dependent kinase 120	CDK120	1.75	5.57E-05
CDK121	749	cyclin dependent kinase 121	CDK121	1.75	5.57E-05
CDK122	750	cyclin dependent kinase 122	CDK122	1.75	5.57E-05
CDK123	751	cyclin dependent kinase 123	CDK123	1.75	5.57E-05
CDK124	752	cyclin dependent kinase 124	CDK124	1.75	5.57E-05
CDK125	753	cyclin dependent kinase 125	CDK125	1.75	5.57E-05
CDK126	754	cyclin dependent kinase 126	CDK126	1.75	5.57E-05
CDK127	755	cyclin dependent kinase 127	CDK127	1.75	5.57E-05
CDK128	756	cyclin dependent kinase 128	CDK128	1.75	5.57E-05
CDK129	757	cyclin dependent kinase 129	CDK129	1.75	5.57E-05
CDK130	758	cyclin dependent kinase 130	CDK130	1.75	5.57E-05
CDK131	759	cyclin dependent kinase 131	CDK131	1.75	5.57E-05
CDK132	760	cyclin dependent kinase 132	CDK132	1.75	5.57E-05
CDK133	761	cyclin dependent kinase 133	CDK133	1.75	5.57E-05
CDK134	762	cyclin dependent kinase 134	CDK134	1.75	5.57E-05
CDK135	763	cyclin dependent kinase 135	CDK135	1.75	5.57E-05
CDK136	764	cyclin dependent kinase 136	CDK136	1.75	5.57E-05
CDK137	765	cyclin dependent kinase 137	CDK137	1.75	5.57E-05
CDK138	766	cyclin dependent kinase 138	CDK138	1.75	5.57E-05
CDK139	767	cyclin dependent kinase 139	CDK139	1.75	5.57E-05
CDK140	768	cyclin dependent kinase 140	CDK140	1.75	5.57E-05
CDK141	769	cyclin dependent kinase 141	CDK141	1.75	5.57E-05
CDK142	770	cyclin dependent kinase 142	CDK142	1.75	5.57E-05
CDK143	771	cyclin dependent kinase 143	CDK143	1.75	5.57E-05
CDK144	772	cyclin dependent kinase 144	CDK144	1.75	5.57E-05
CDK145	773	cyclin dependent kinase 145	CDK145	1.75	5.57E-05
CDK146	774	cyclin dependent kinase 146	CDK146	1.75	5.57E-05
CDK147	775	cyclin dependent kinase 147	CDK147	1.75	5.57E-05
CDK148	776	cyclin dependent kinase 148	CDK148	1.75	5.57E-05
CDK149	777	cyclin dependent kinase 149	CDK149	1.75	5.57E-05
CDK150	778	cyclin dependent kinase 150	CDK150	1.75	5.57E-05
CDK151	779	cyclin dependent kinase 151	CDK151	1.75	5.57E-05
CDK152	780	cyclin dependent kinase 152	CDK152	1.75	5.57E-05
CDK153	781	cyclin dependent kinase 153	CDK153	1.75	5.57E-05
CDK154	782	cyclin dependent kinase 154	CDK154	1.75	5.57E-05
CDK155	783	cyclin dependent kinase 155	CDK155	1.75	5.57E-05
CDK156	784	cyclin dependent kinase 156	CDK156	1.75	5.57E-05
CDK157	785	cyclin dependent kinase 157	CDK157	1.75	5.57E-05
CDK158	786	cyclin dependent kinase 158	CDK158	1.75	5.57E-05
CDK159	787	cyclin dependent kinase 159	CDK159	1.75	5.57E-05
CDK160	788	cyclin dependent kinase 160	CDK160	1.75	5.57E-05
CDK161	789	cyclin dependent kinase 161	CDK161	1.75	5.57E-05
CDK162	790	cyclin dependent kinase 162	CDK162	1.75	5.57E-05
CDK163	791	cyclin dependent kinase 163	CDK163	1.75	5.57E-05
CDK164	792	cyclin dependent kinase 164	CDK164	1.75	5.57E-05
CDK165	793	cyclin dependent kinase 165	CDK165	1.75	5.57E-05
CDK166	794	cyclin dependent kinase 166	CDK166	1.75	5.57E-05
CDK167	795	cyclin dependent kinase 167	CDK167	1.75	5.57E-05
CDK168	796	cyclin dependent kinase 168	CDK168	1.75	5.

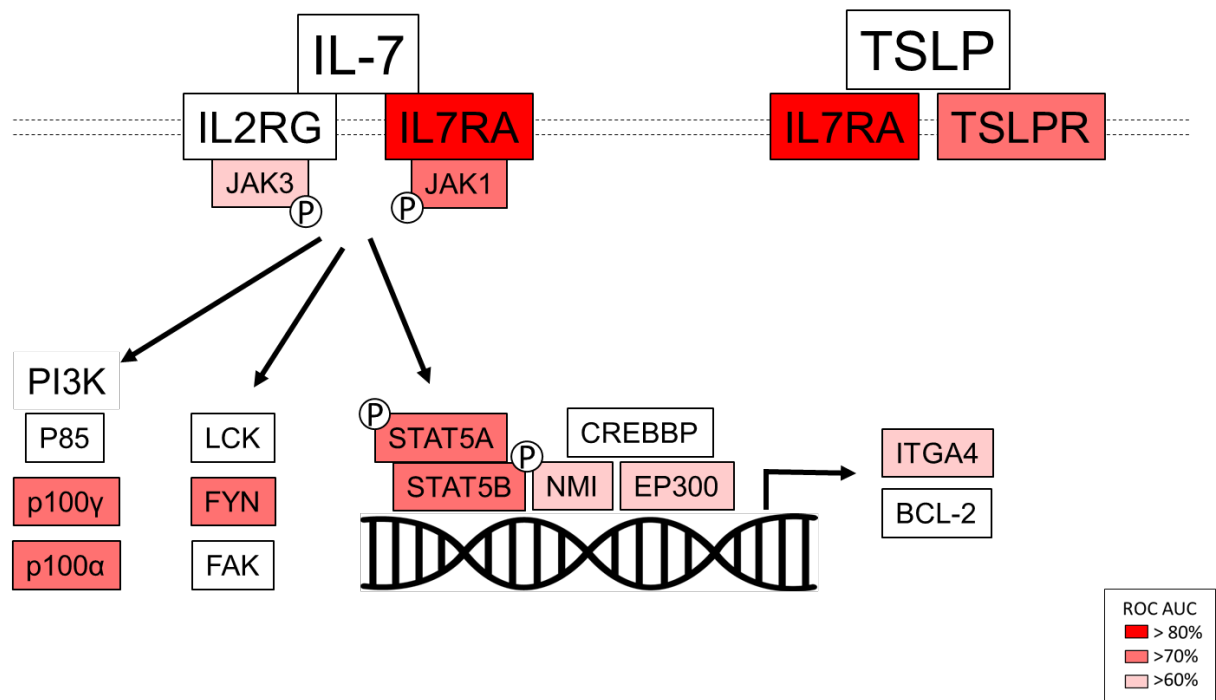
Supplementary Figure 4: Differential gene expression between colon mucosa of responders and non-responders UC patients before therapy with anti-TNF.

(a) Heatmap of the expression of all genes in colon biopsies of non-IBD controls (n=18), responders (green, n=28) and non-responders (red, n=41) before anti-TNF therapy and identification of a cluster of 1698 genes including *IL7R*. Meta-analysis of 3 UC cohorts with histological healing as the anti-TNF response criteria: dataset GSE16879 (43) and GSE12251 (44), and GSE73661 (46). (b) Mean expression profile of the *IL7R* cluster in same group as in (a). (c) Gene Ontology (GO) identified, with the *ClusterProfiler* R package, in the *IL7R* cluster as in (a). Circle size is proportional to the number of genes for each category. Circle color is related to adjusted p-value.

Supplementary figure 4

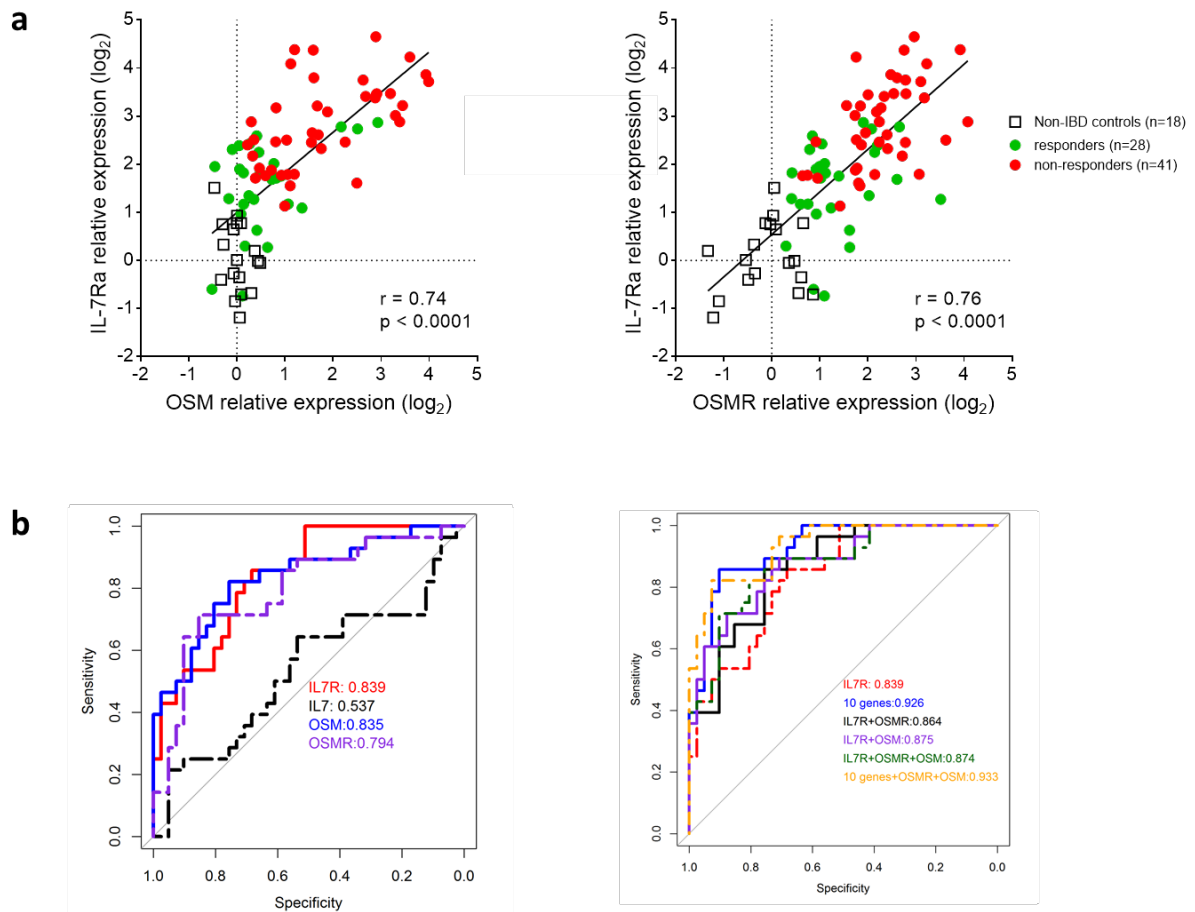


Supplementary Figure 5: IL7R pathway annotation based on gene expression in colon biopsies of UC patients with unresponsiveness before initiation of anti-TNF treatment.
Colorization according ROC AUC values in the meta-analysis in Figure 2.



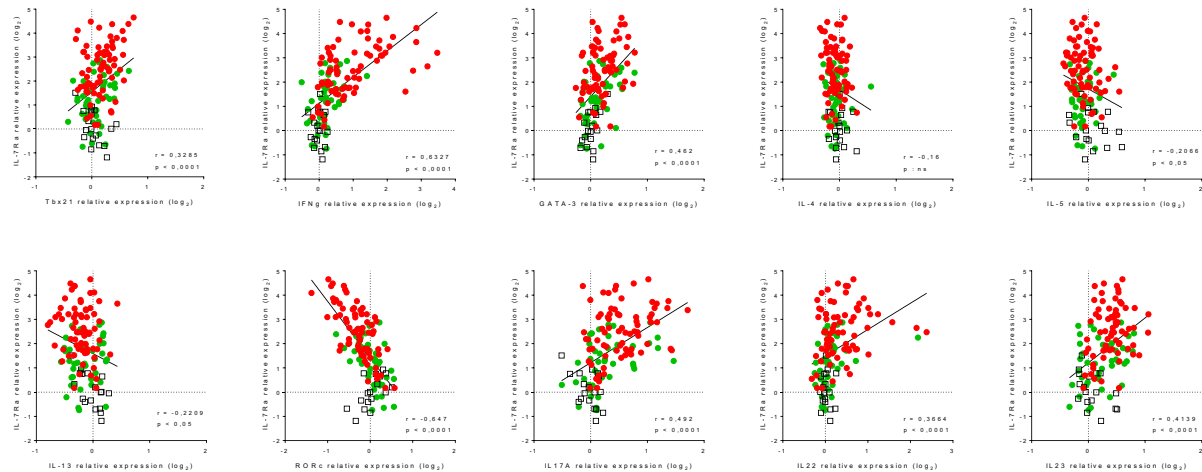
Supplementary Figure 6: *IL7R* correlation with *OSM* and *OSMR* expression in colon mucosa of responders and non-responders UC patients before therapy with anti-TNF.

(a) Correlative analysis between *IL7R* and *OSM* (Left) or *OSMR* (Right) relative gene expression before anti-TNF treatment (log₂ data normalized to control median) in colon mucosa of UC patients and non-IBD controls. (b) ROC (Receiver Operating Characteristic) analysis of *IL7R*, *IL7*, *OSM*, *OSMR* expression, the 10-gene *IL7R*-related signaling signature and some combination distinguishing anti-TNF responders and non-responders in the meta-analysis.



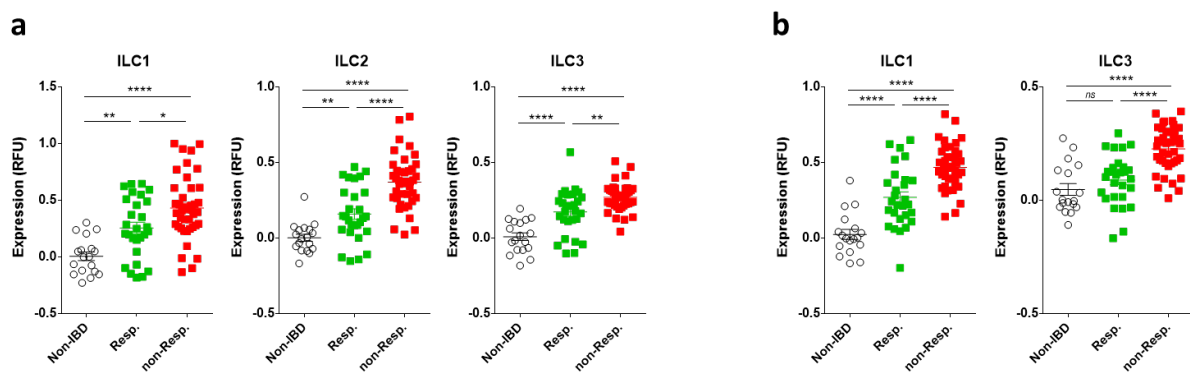
Supplementary Figure 7: IL7R gene expression correlates with Th1 effector cells signature.

Correlative analysis between IL7R α expression and indicated genes considered as hallmark of Th1 (Tbx21, IFN γ), Th2 (GATA3, IL4, IL5, IL13) or Th17 (RORc, IL17A, IL22, IL23) effectors cells (log₂ data normalized to control median) in colon mucosa of UC patients before and after treatment by anti-TNF and in non-IBD controls. Each symbol represents one patient. Linear regression is represented by black lines as well as the Pearson r correlation coefficient with its' p-value.



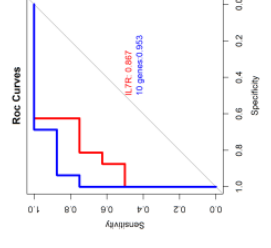
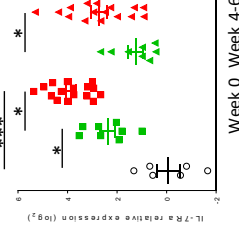
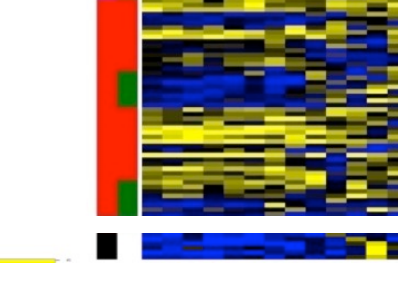
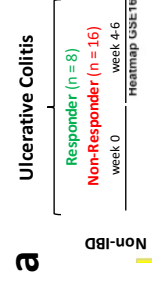
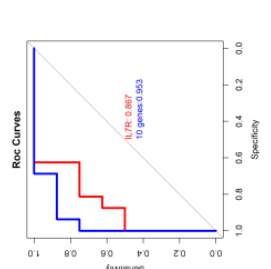
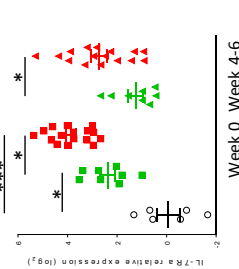
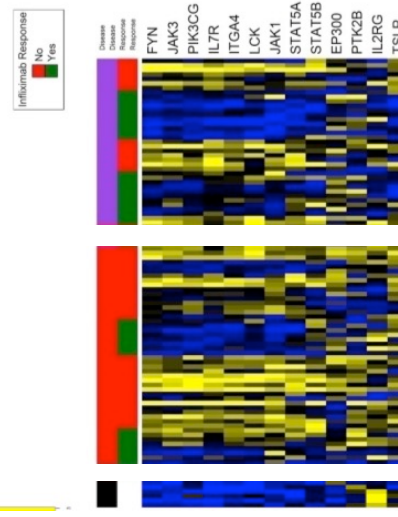
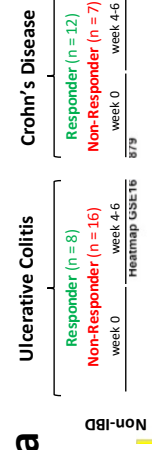
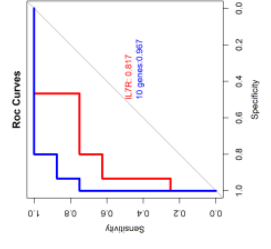
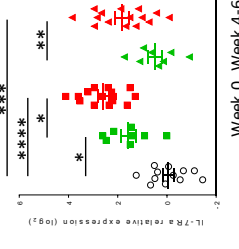
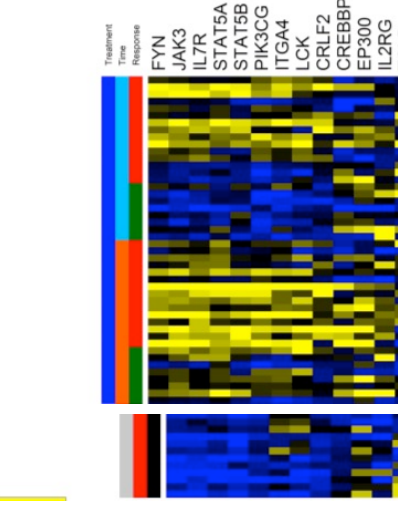
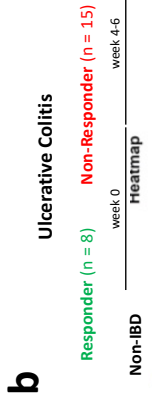
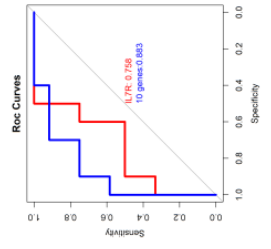
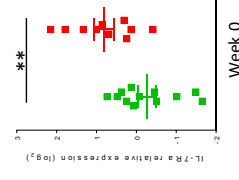
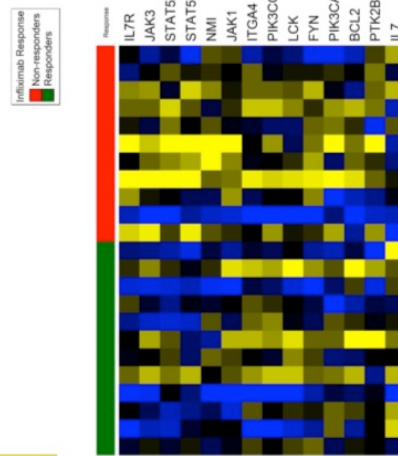
Supplementary Figure 8: Human ILC gene expression signature analysis in colon mucosa of responder and non-responder UC patients before therapy with anti-TNF.

Relative human ILC subsets gene expression signature before anti-TNF treatment (log2 data normalized to control median) in colon mucosa of UC patients and non-IBD controls, using tonsil CD127+ gene expression signatures defined by (a) Björklund et al. (50) or (b) Koues et al. (51) (ILC2 were not analyzed by Koues et al. due to low abundance in tonsils).



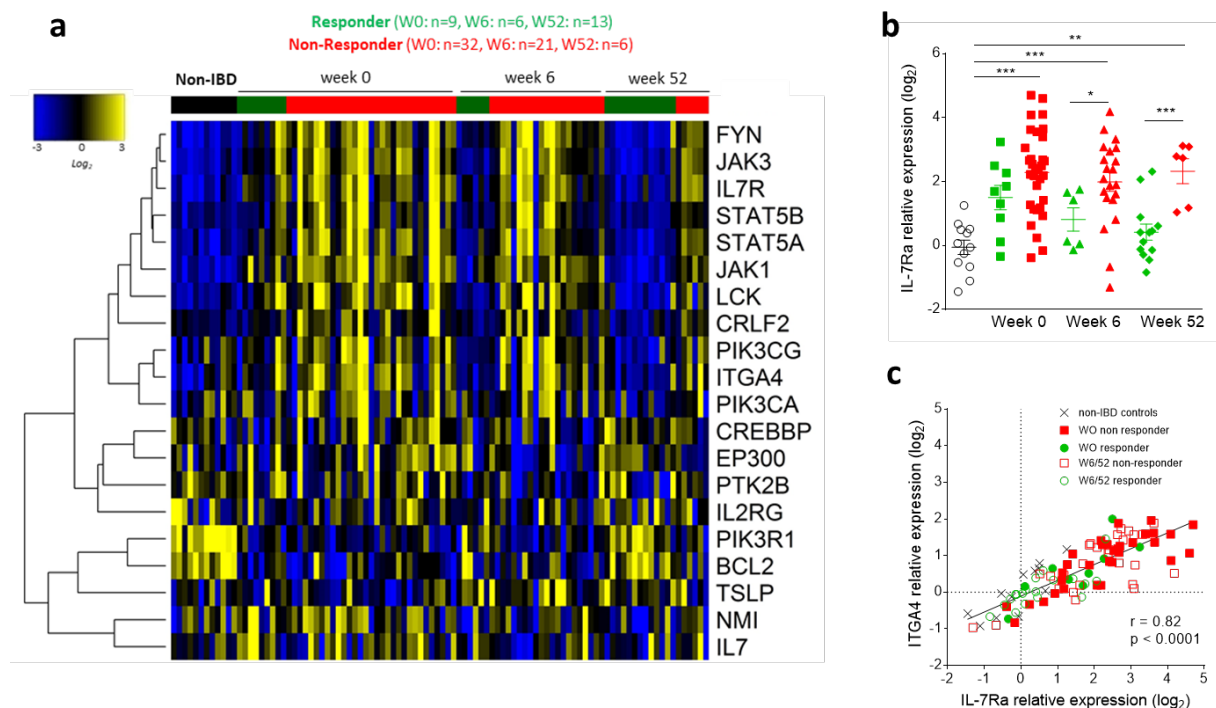
Supplementary Figure 9: IL7R signaling signature in colon biopsies before and after anti-TNF therapy in the 3 individual cohorts of UC used for the meta-analysis and in 1 cohort of CD patients.

(a) Up- Heatmap of the 20 selected genes previously reported as key members of the IL7R signaling pathway (39), in colon biopsies from non-IBD controls (black: n = 6), UC patients (green: responder n = 8, red: non-responder n = 16) and CD patients (green: responder n = 12, red: non-responder n = 7) treated with anti-TNF therapy (dataset GSE16879) (43). Samples were analyzed within a week before anti-TNF infusion and 4-6 weeks after treatment initiation. The heatmap represents median-centered and colorized expression values in which yellow and blue values indicate over-expression and under-expression, respectively. *Middle-* Relative *IL7R* expression before and after anti-TNF treatment (log2 data normalized to control median). *Bottom-* ROC (Receiver Operating Characteristic) analysis of *IL7R* expression and the 10-gene IL7R-related signaling signature distinguishing anti-TNF responders and non-responders in this dataset. **(b) Up-** Heatmap of the IL7R signaling signature (20 selected genes) in colon biopsies from non-IBD controls (black: n = 12) and UC patients (green: responder n = 8, red: non-responder n = 15) treated with anti-TNF therapy (dataset GSE73661⁶). *Middle-* Relative *IL7R* expression before and after anti-TNF treatment (log2 data normalized to control median). *Bottom-* ROC analysis of *IL7R* expression and the 10-gene IL7R-related signaling signature distinguishing anti-TNF responders and non-responders in this dataset. **(c) Up-** Heatmap of the IL7R signaling signature (20 selected genes) in colon biopsies from UC patients (green: responder n = 12, red: non-responder n = 10) before treatment with anti-TNF therapy (dataset GSE12251⁵). *Middle-* Relative *IL7R* expression before anti-TNF treatment (log2 data normalized to control median). *Bottom-* ROC analysis of *IL7R* expression and the 10-gene IL7R-related signaling signature distinguishing anti-TNF responders and non-responders in this dataset. * p<0.05; ** p<0.01; *** p<0.001, **** p<0.0001 between indicated groups.



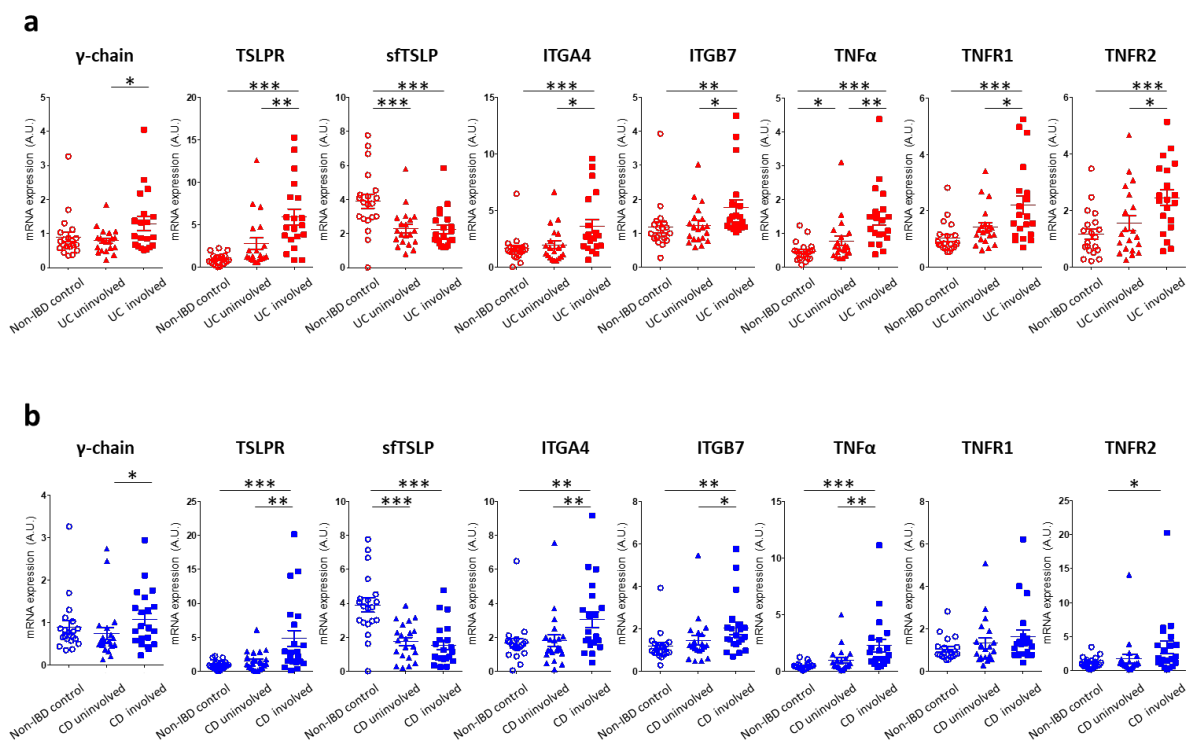
Supplementary Figure 10: IL7R signaling signature in colon biopsies before and after anti- α 4 β 7 (Vedolizumab) therapy in UC patients.

(a) Heatmap of the 20 selected genes previously reported as key members of the IL7R signaling pathway (39), in colon biopsies from non-IBD controls (black: n = 12) and UC patients (green: responder n = 9-13, red: non-responder n = 6-32) treated with anti- α 4 β 7 therapy (dataset GSE73661) (46). Samples were analyzed before anti- α 4 β 7 infusion as well as 6 or 52 weeks after treatment initiation. The heatmap represents median-centered and colorized expression values in which yellow and blue values indicate over-expression and under-expression, respectively. (b) Relative *IL7R* expression before and after anti- α 4 β 7 treatment (log₂ data normalized to control median). (c) Correlative analysis between *IL7R* and *ITGA4* relative gene expression before anti-TNF treatment (log₂ data normalized to control median) in colon mucosa of UC patients and non-IBD controls. * p<0.05; ** p<0.01; *** p<0.001 between indicated groups.



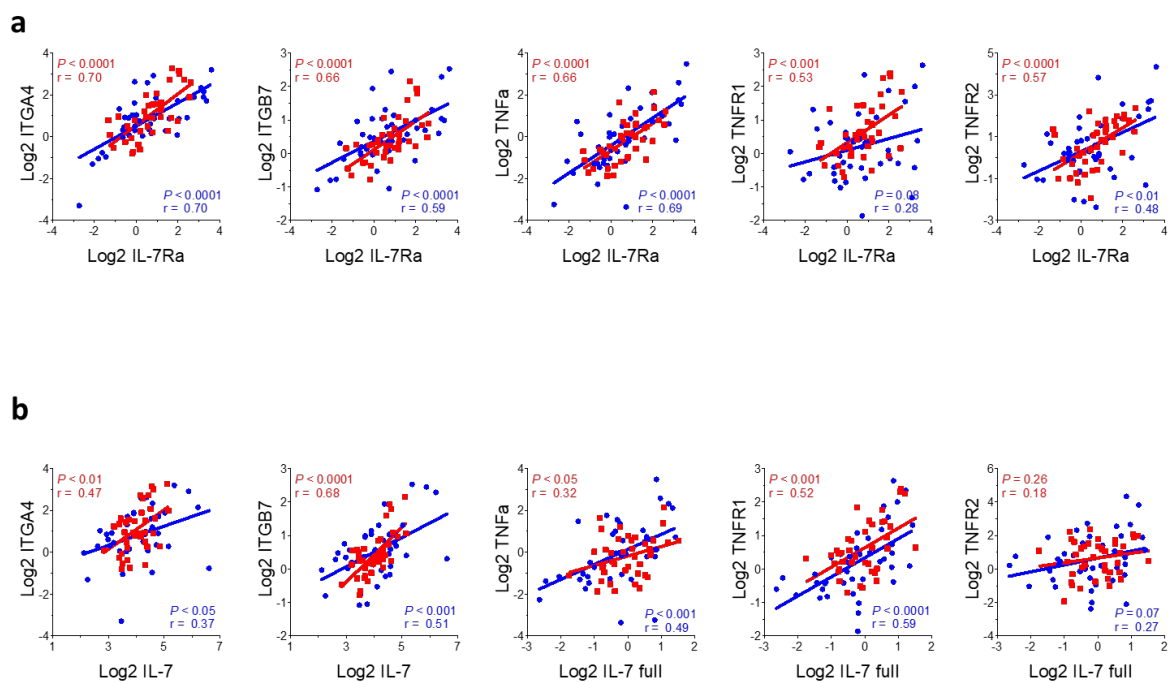
Supplementary Figure 11: mRNA expression of the TSLP, $\alpha 4\beta 7$ and TNF pathway in IBD biopsies.

Relative expression of indicated genes, as measured by reverse transcriptase polymerase chain reaction (RT-PCR) of colon biopsies (same as Figure 1) from inflamed and the healthy area of (a) Ulcerative Colitis (UC, n=21) and (b) Crohn's Disease (CD, n=24) patients as compared to non-IBD controls patients (n=20). Each symbol represents one patient, bars represent means and error bars show SEM. * p<0.05; ** p<0.01; *** p<0.001 between indicated groups.



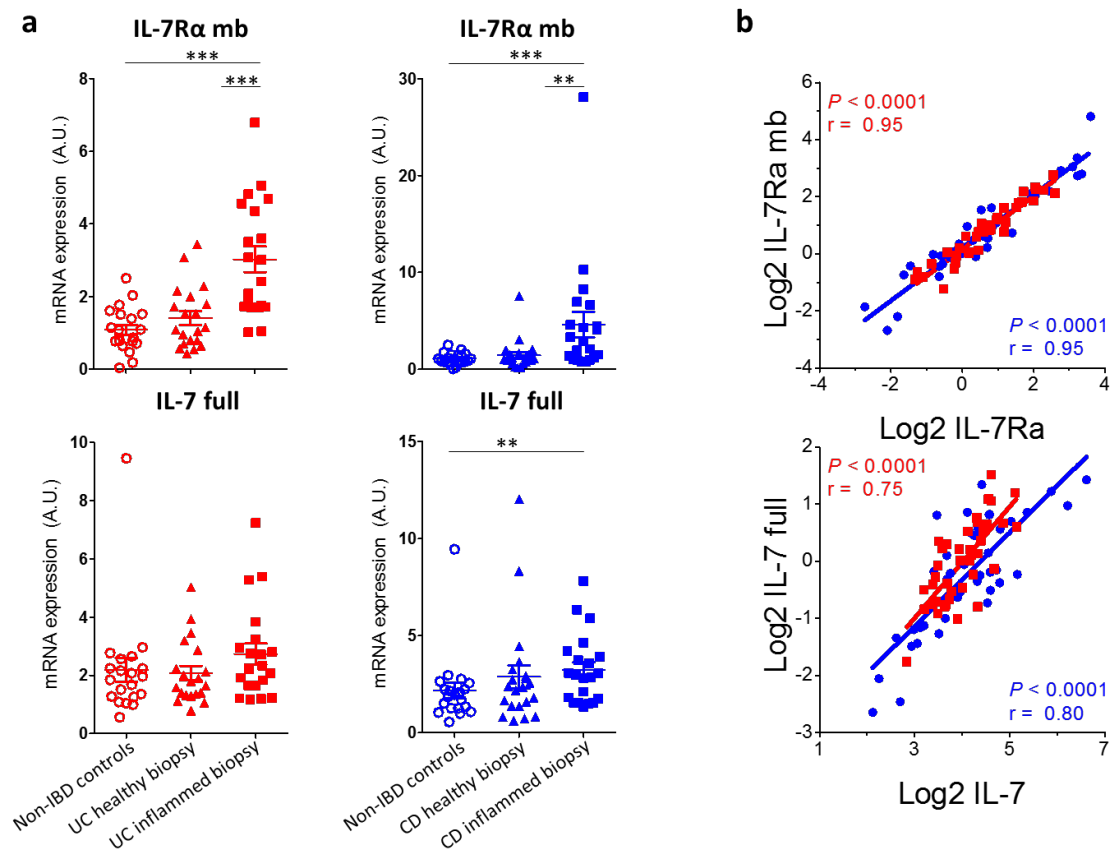
Supplementary Figure 12: IL7/IL7R α mRNA expression correlates with α 4 β 7 and TNF pathway mRNA expression in IBD biopsies.

(a) Correlative analysis between IL7R α and integrin α 4 (*ITGA4*) or integrin β 7 (*ITGB7*), TNF, TNFR1 or TNFR2 relative gene expression in the same UC (red) and CD (blue) patients as described in Supplementary Figure 9. Each symbol represents one patient. Linear regression is represented by respective colored lines as well as the Pearson r correlation coefficient with its' p-value. (b) same as in (a) for IL7 gene expression correlation with same gene.



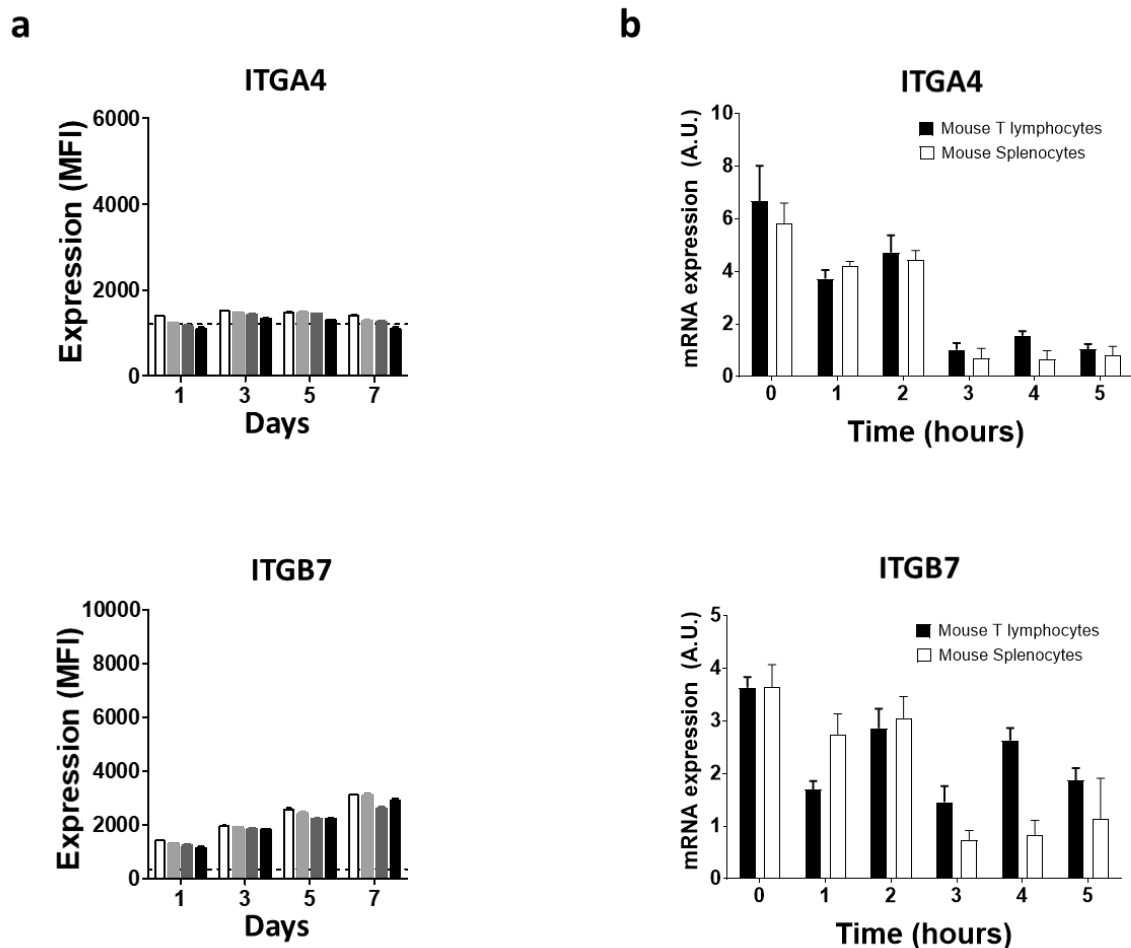
Supplementary Figure 13: Full-length IL7 and membrane IL7R α mRNA isoform expression in IBD biopsies.

(a) Relative full-length IL7 and membrane IL7R α (IL7R α mb) gene isoform expression, as measured by reverse transcriptase polymerase chain reaction (RT-PCR) of colon biopsies (same as Figure 1) from inflamed and healthy areas of Ulcerative Colitis (UC, red, n=21) and Crohn's Disease (CD, blue, n=24) patients as compared to non-IBD control patients (n=20). Each symbol represents one patient, bars represent means and error bars show SEM. * $p < 0.05$; ** $p < 0.01$; *** $p < 0.001$ between indicated groups. (b) Correlative gene expression analysis between membrane IL7R α and all IL7R α isoforms (up) as well as full-length IL7 and all IL7 isoforms (bottom) in the same UC (red) and CD (blue) patients as described in (a). Each symbol represents one patient. Linear regression is represented by respective colored lines as well as the Pearson r correlation coefficient with its' p -value.



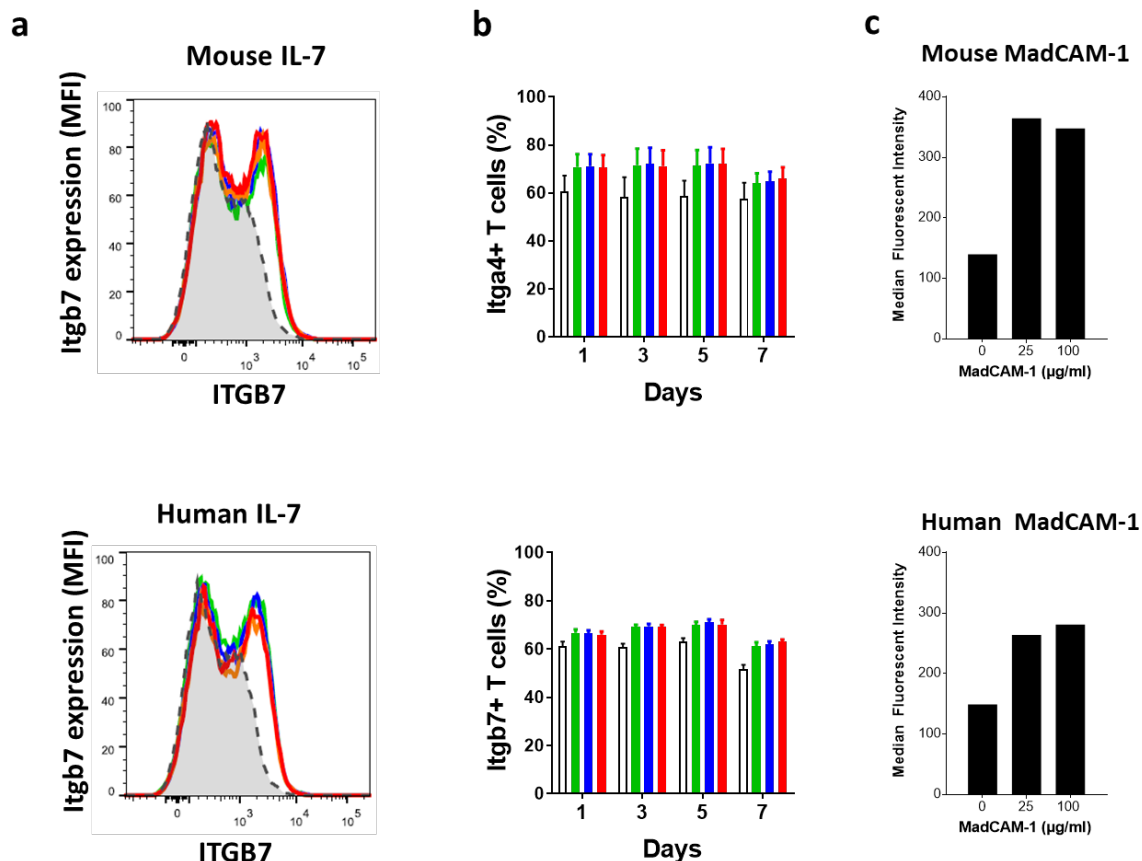
Supplementary Figure 14: $\alpha 4\beta 7$ expression on mouse T lymphocytes is not controlled by IL7

(a) Integrin $\alpha 4$ and $\beta 7$ surface expression on mouse T lymphocytes cultured for the indicated period of time in medium alone (white bars) or supplemented with recombinant mouse IL7 at 1ng/ml (light grey), 5ng/ml (dark grey) or 25ng/ml (black). Data are expressed as median fluorescent intensity (MFI) \pm SEM measured by flow cytometry. (b) Integrin $\alpha 4$ (ITGA4) and $\beta 7$ (ITGB7) mRNA expression in mouse T lymphocytes (black) or total splenocytes (white) cultured for the indicated period of time with 25ng/ml of mouse recombinant IL7. Data are mean \pm SEM of 3 experiments.



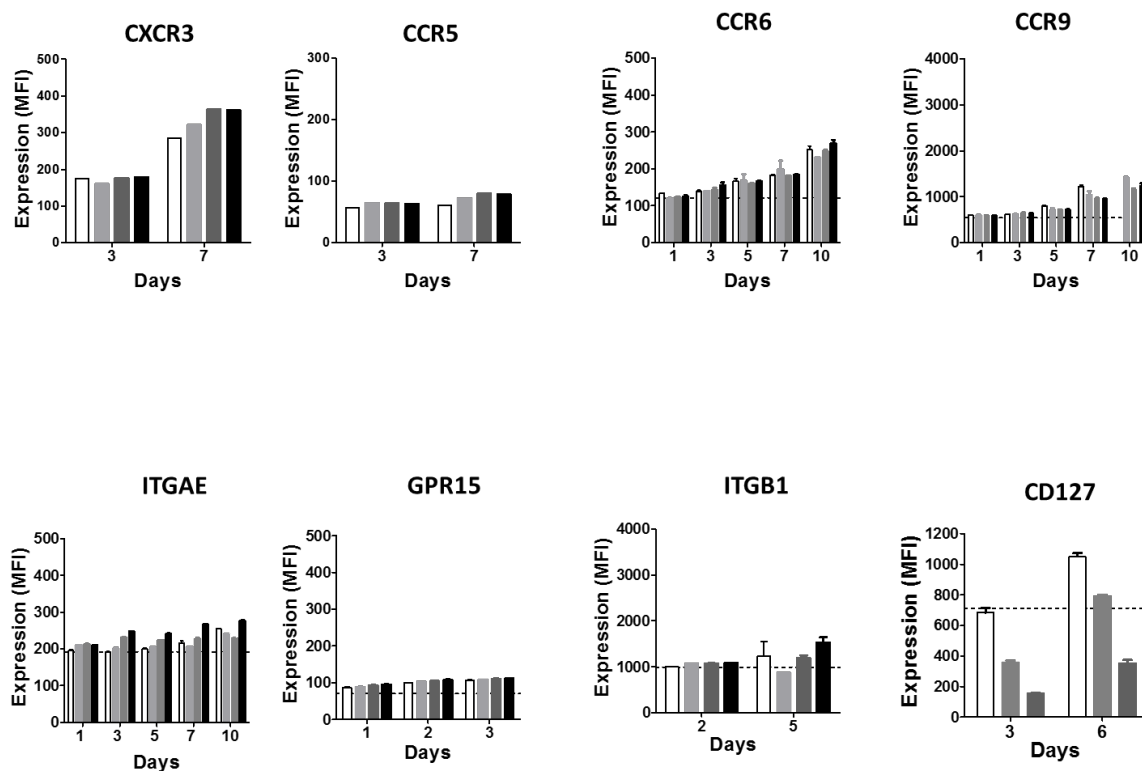
Supplementary Figure 15: IL7/IL7R α and α 4 β 7/MADCAM1 compatibilities between mouse and human species

(a) β 7 integrin expression on human T lymphocytes cultured 48 hours with mouse (*Up*) or human (*Bottom*) recombinant IL7 at 10ng/ml (red), 25ng/ml (green), 50ng/ml (blue) or 75ng/ml (orange). Dotted line represents basal expression at t0. Data shows one representative of 3 experiments. (b) Integrin α 4 (*Up*) and β 7 (*Bottom*) positive human T lymphocytes after culture with the indicated period of time in medium alone (white bars) or supplemented with recombinant human IL7 at 1ng/ml (green), 5ng/ml (blue) or 25ng/ml (red). Data are expressed as mean \pm SEM measured by flow cytometry (n=6). (c) Mouse MADCAM1 (*Up*) and human MADCAM1 (*Bottom*) binding on α 4 β 7+ human T lymphocytes.



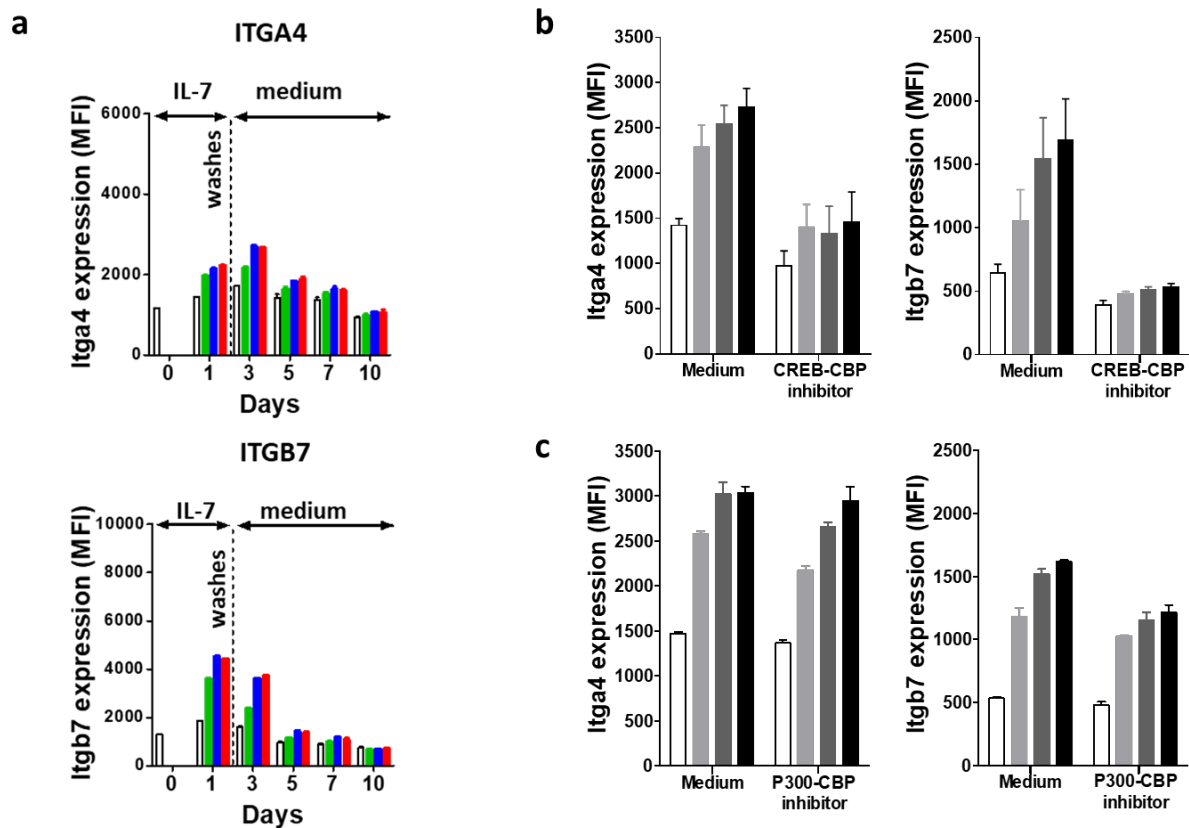
Supplementary Figure 16: IL7 does not control expression of other gut-specific integrin or chemokine receptors on human T lymphocytes.

Surface expression of indicated proteins on human T lymphocytes from the blood of healthy volunteers cultured for the indicated period of time in medium alone (white bars) or supplemented with recombinant human IL7 at 1ng/ml (light grey), 5ng/ml (dark grey) or 25ng/ml (black). Data are expressed as median fluorescent intensity (MFI) \pm SEM measured by flow cytometry. Dotted line represents basal expression at t0. Data shows one representative of 3 experiments.



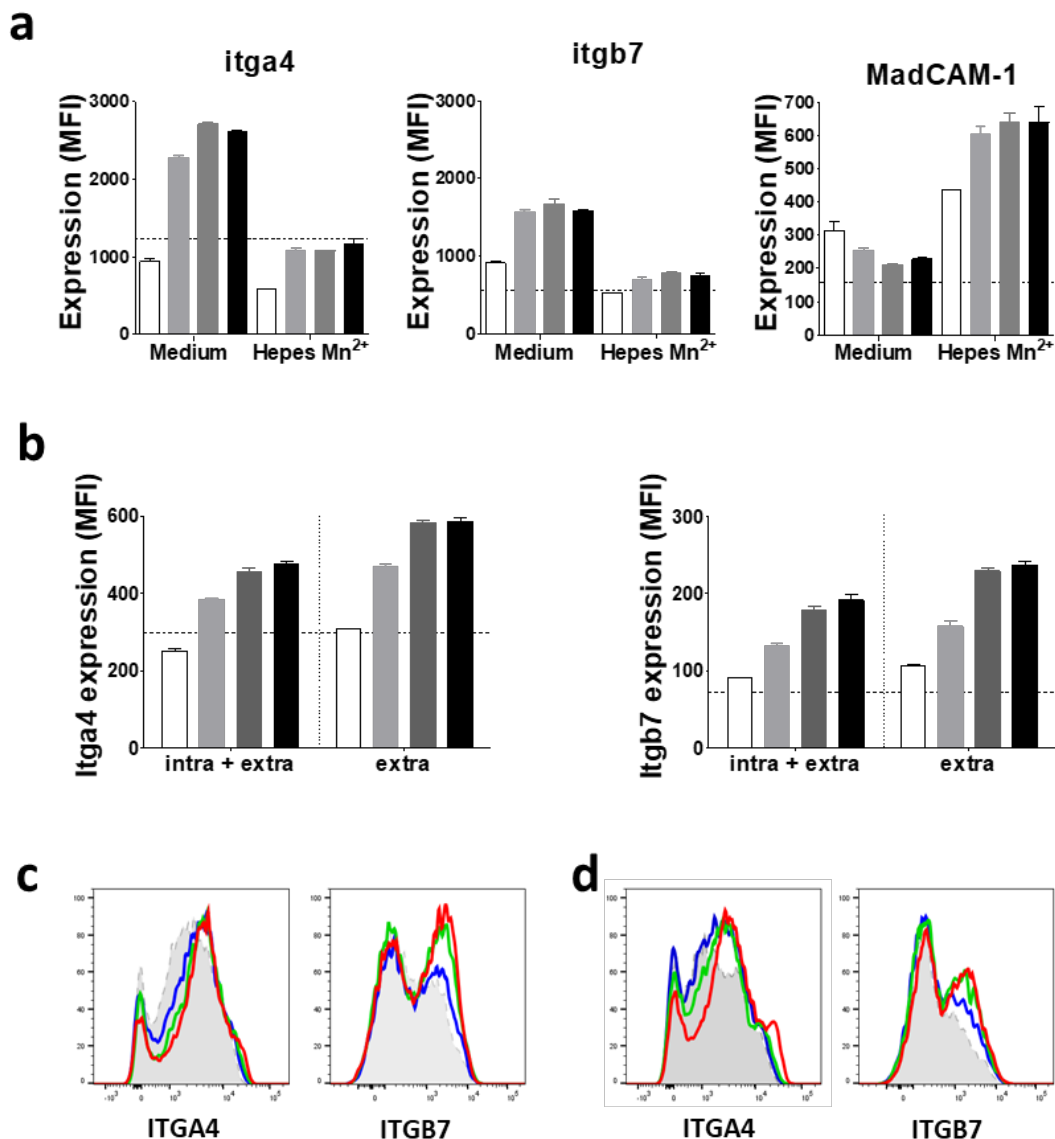
Supplementary Figure 17: IL7 controls $\alpha4\beta7$ expression through the CREB transcription factor as well as JAK/STAT and PI3K pathways.

(a) Integrin $\alpha4$ and $\beta7$ surface expression on human T lymphocytes from the blood of healthy volunteers cultured for 24 hours in medium alone (white bars) or supplemented with recombinant human IL7 at 1ng/ml (green), 5ng/ml (blue) or 25ng/ml (red). Cells were then washed to remove IL7 and were then cultured with medium alone for the indicated time. Data are expressed as median fluorescent intensity (MFI) \pm SEM measured by flow cytometry. (b) Integrin $\alpha4$ and $\beta7$ surface expression on human T lymphocytes cultured for 48 hours with or without 10nM of CREB/CBP interaction inhibitor or (c) 10nM of CBP/P300 histone acetyltransferase inhibitor in medium alone (white bars) or supplemented with recombinant human IL7 at 1ng/ml (light grey), 5ng/ml (dark grey) or 25ng/ml (black). Data are expressed as median fluorescent intensity (MFI) \pm SEM of three experiments measured by flow cytometry.



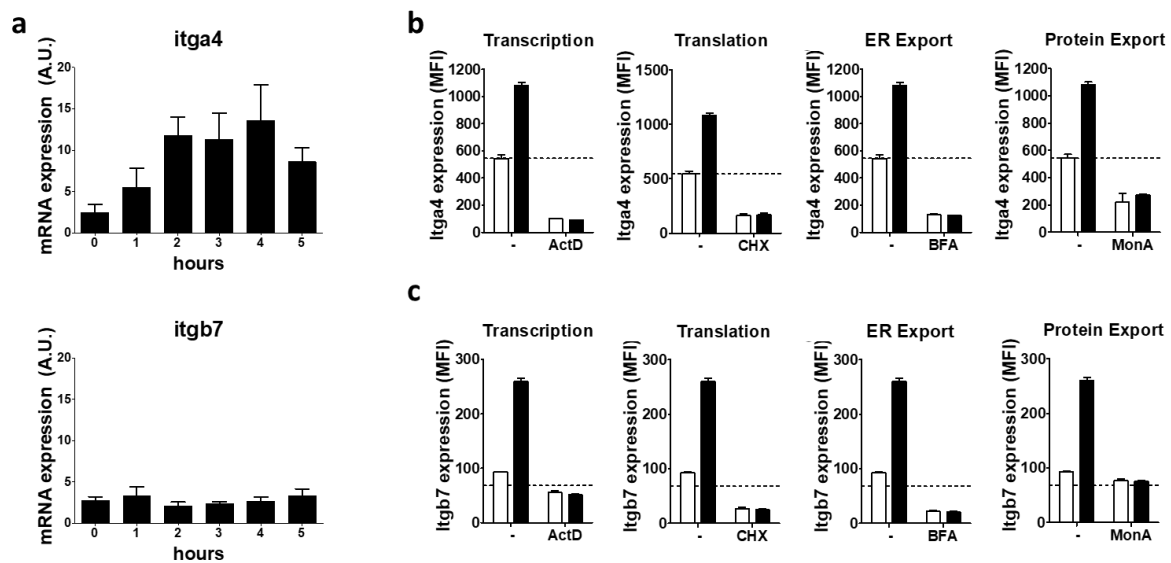
Supplementary Figure 18: IL7 controls ITGA4 transcription and ITGB7 translation.

(a) Integrin $\alpha 4$, $\beta 7$ surface staining and MADCAM1 binding on human T lymphocytes from the blood of healthy volunteers cultured for 48 hours in medium alone (white bars) or supplemented with recombinant human IL7 at 1ng/ml (light grey), 5ng/ml (dark grey) or 25ng/ml (black). Data are expressed as median fluorescent intensity (MFI) \pm SEM measured by flow cytometry. Cells were then stained in classic media or Hepes Mn²⁺ buffer to allow $\alpha 4/\beta 7$ conformational change required to evaluate MADCAM1 binding. Dotted line represents basal staining at t0. (b) Same as in (a) but integrin $\alpha 4$ and $\beta 7$ expression was evaluated on permeabilized or non-permeabilized T cells before staining. Representative FACS profile of extracellular (c) and intracellular + extracellular (d) staining of ITGA4 and ITGB7 on human T-cell cultured as in (a) with IL7 at 0 ng/ml (grey), 1ng/ml (blue line), 5ng/ml (green line) or 25ng/ml (red line).



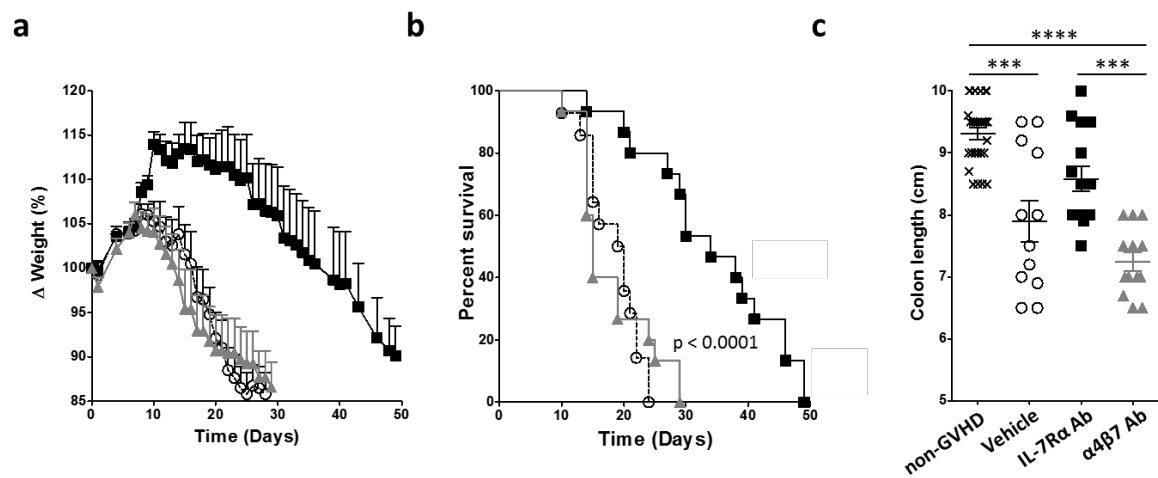
Supplementary Figure 19: IL7 controls ITGA4 transcription and ITGB7 translation.

(a) Integrin $\alpha 4$ (up) and $\beta 7$ (bottom) mRNA quantification isolated from human T cells cultured for the indicated period of time with or without 5ng/ml of human IL7 and evaluated by RT-qPCR. (b) Integrin $\alpha 4$ and (c) Integrin $\beta 7$ surface expression on human T lymphocytes cultured for 24 hours with (black bars) or without (white bars) 1ng/ml of human IL7 and when indicated with 100ng/ml of Actinomycin D (ActD) transcription inhibitor, 100ng/ml of Cycloheximide (CHX) translation inhibitor, 10ng/ml of Brefeldin A (BFA) endoplasmic reticulum (ER) export inhibitor or 100ng/ml of Monensin A (MonA) membrane protein export inhibitor. Data are expressed as median fluorescent intensity (MFI) \pm SEM measured by flow cytometry. Dotted line represents basal staining at t0.



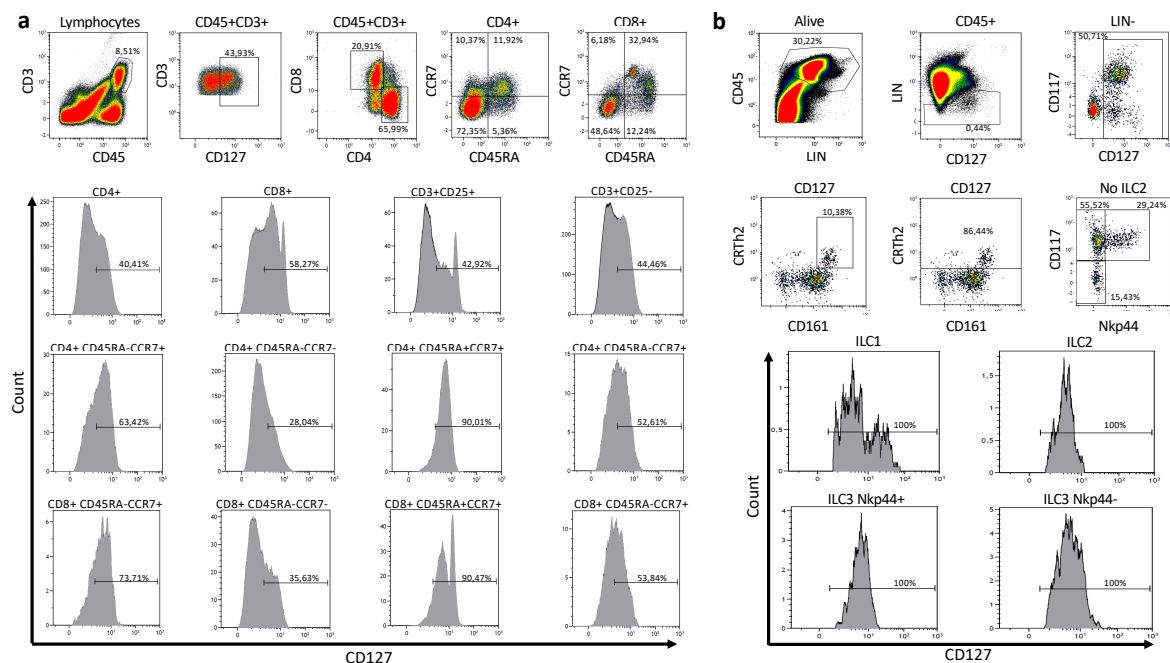
Supplementary Figure 20: IL7R α blockade differs from anti- α 4 β 7 mAb in controlling GVHD and colon inflammation in humanized mice.

(a) Weight variation (mean \pm SEM), (b) survival and (c) colon length of immunodeficient NOD/scid IL-2R $\gamma^{-/-}$ (NSG) mice reconstituted with 50×10^6 freshly purified human PBMC from healthy donors and treated three times per week for 4 weeks from day 0 with control vehicle (\circ , n=14), 5mg/Kg of blocking anti-human IL7R α mAb (\blacksquare , n=15) or blocking anti-human α 4 β 7 (Vedolizumab) mAb (\blacktriangle , n=15). Colon length was measured for each mouse after losing 20% of body weight, except for the non-GVHD control group (\times , n=23) which includes control NSG mice used for non-GVHD experiments. Each symbol represents one mouse, horizontal bars mean \pm SEM. *** p<0.001; **** p<0.0001.



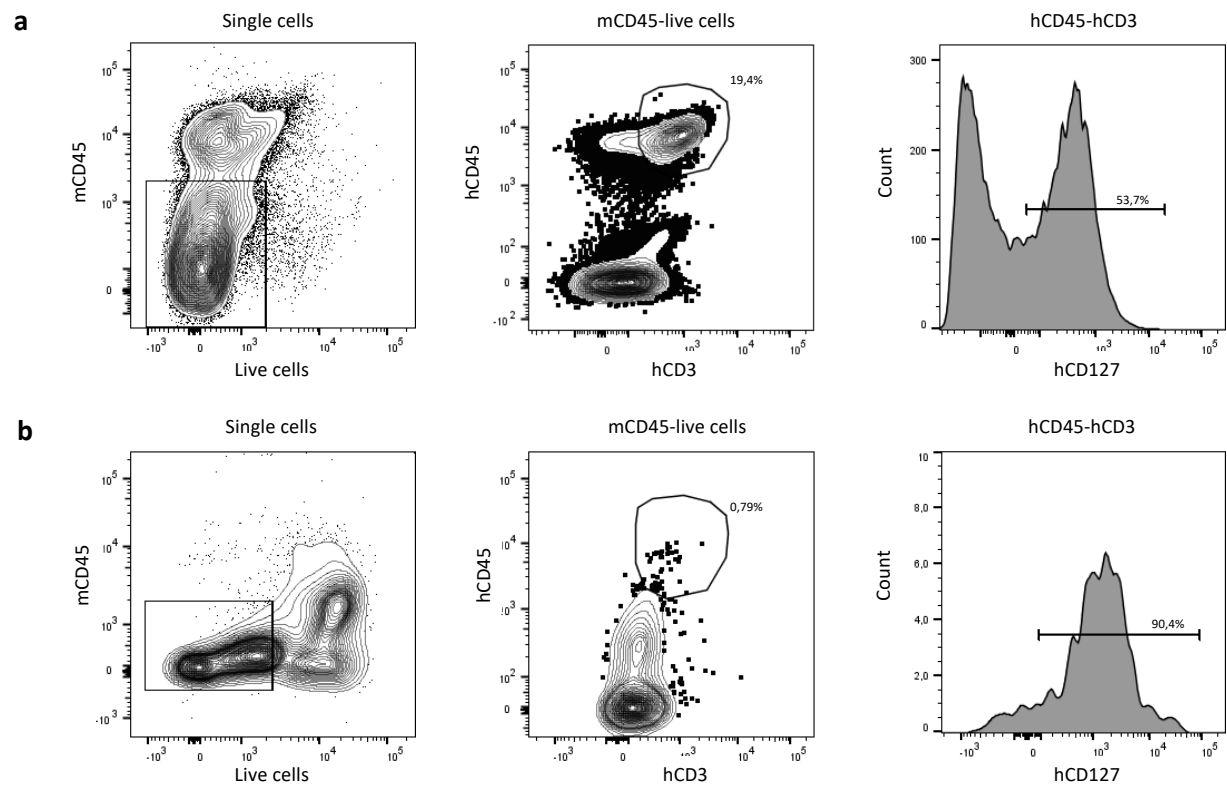
Supplementary Figure 21: IL7R α expression by spleen T-lymphocytes and ILCs subsets in humanized mice reconstituted with CD34+ hematopoietic stem cells.

Representative flow cytometry profile from the spleen of a humanized mouse reconstituted 4 months earlier with 50×10^3 human cord blood CD34+ hematopoietic stem cells. **(a)** Human T-cells were analyzed using anti-human CD45 and CD3 fluorescent antibody. T-cells subsets were determined using CD4 vs CD8 expression, CD4+ CD25+ T cells (which contained mainly human Tregs) as well as CCR7 and CD45RA markers defining naïve (CCR7+ CD45RA+), central memory (CCR7+ CD45RA-), effector memory (CCR7- CD45RA-) and CD45RA re-expressing memory cells (CCR7- CD45RA+). **(b)** ILCs subsets were determined within human CD45+ lineage negative cells and using the CD127 marker. ILCs subsets were determined in this rare lineage⁻ CD127⁺ human cells by the expression of CRTH2 and CD161 for ILC2, the lack of CRTH2 and CD117 expression for ILC1 and the lack of CRTH2 plus the expression of CD117 for ILC3 expressing or not Nkp44. The level of CD127 expression was analyzed in each subset.



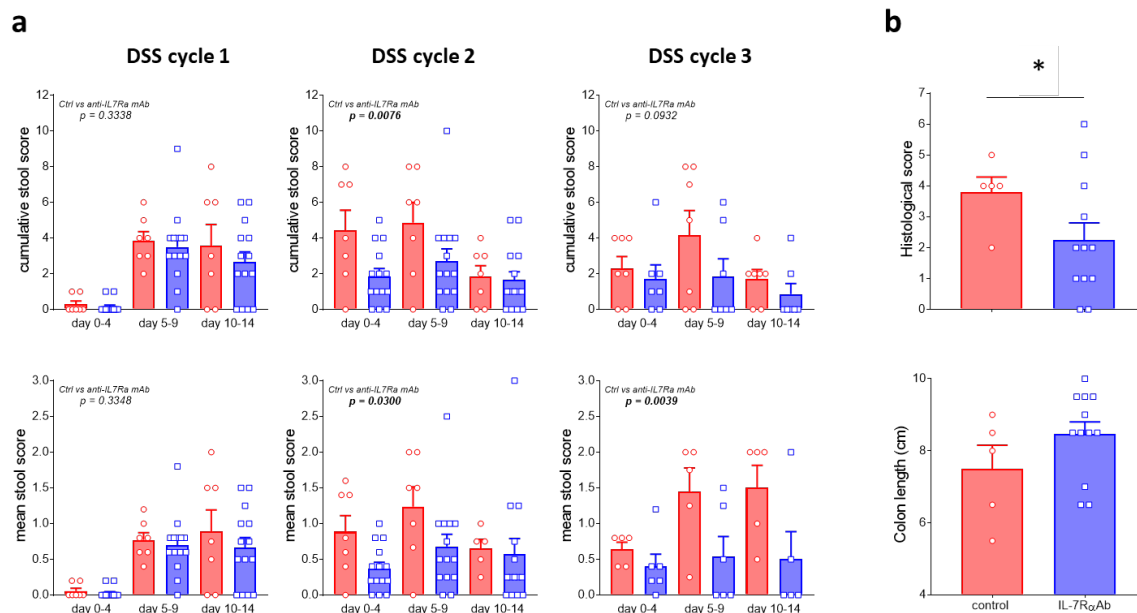
Supplementary Figure 22: Human T lymphocytes in the colon of humanized mice express IL7R α .

Representative flow cytometry profile from the spleen (a) and colon (b) of a humanized mouse reconstituted 4 months earlier with 50×10^3 human cord blood CD34+ hematopoietic stem cells. Human T-cells were analyzed within live cells by eliminating mouse CD45+ leukocytes and then expression of human CD45 and human CD3 markers. The level of CD127 expression was analyzed in spleen and lamina propria human T lymphocytes.



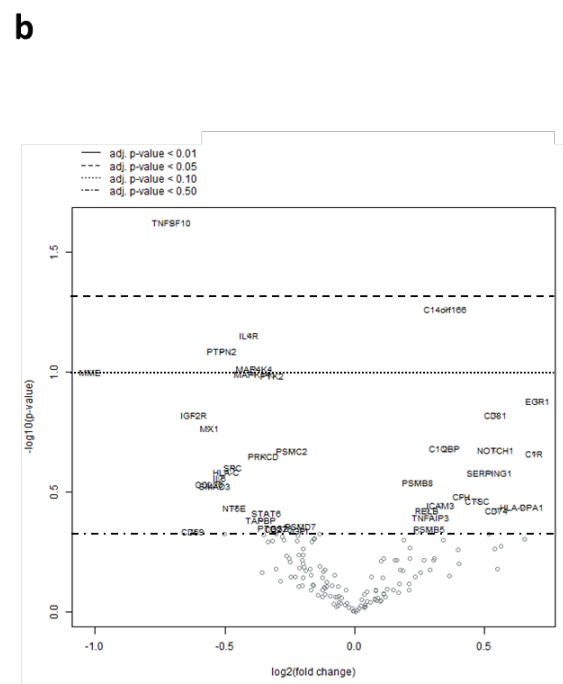
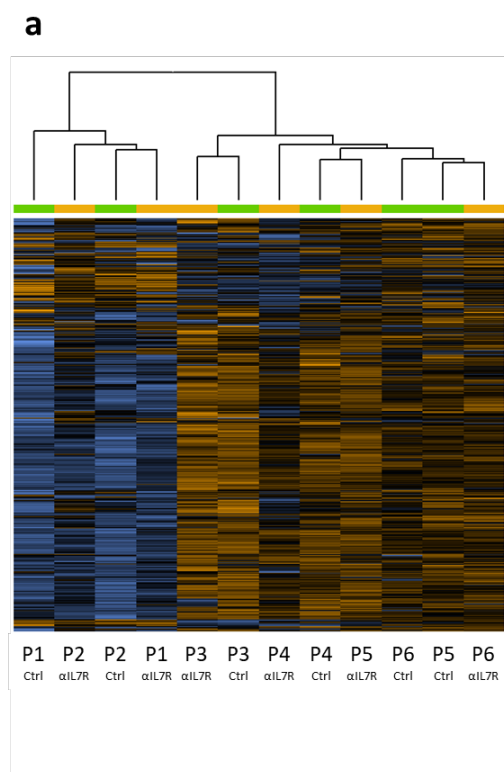
Supplementary Figure 23: *IL7R α* blockade efficiency *in-vivo* in humanized chronic DSS colitis.

NSG mice previously reconstituted (at day -7) with 2.5×10^6 freshly purified human PBMC from healthy donors after total mouse body irradiation at 1.5 gray, received every other week 1% of Dextran Sulfate Sodium (DSS) in drinking water for 3 cycles. Mice were treated intraperitoneally three times per week with 5mg/Kg of blocking anti-human *IL7R α* mAb (blue) or vehicle (red) at the beginning of the second DSS cycle. (a) Cumulative (*Up*) and mean (*Bottom*) colitis stool score were reported for the beginning (day 0-4), middle (day 5-9) and end (day 10-14) of each cycle. p-value between control (vehicle) and anti- human *IL7R α* treatment was calculated using two-way ANOVA statistical test. (b) Colon histological score (*Up*) and colon length (*Bottom*) examined two weeks after the beginning of the third DSS cycle. * $p < 0.05$ between indicated groups.



Supplementary Figure 24: Nanostring analysis of IL7R α blockade *ex-vivo* in human UC organ cultures.

(a) Clustering on the Heatmap analysis of the of 255 genes of the Nanostring human transcriptional inflammation panel performed on Ulcerative Colitis (UC, n=6) inflamed colon fragments cultured *ex-vivo* at 37°C for 24 hours in medium with 10 μ g/ml of IgG control mAb or blocking anti-human IL7R α mAb. Samples from the same patients (P) were cultured with IgG control or anti-IL7R α mAbs. (b) Volcano Plot of the differential expression in anti-IL7R α versus baseline of isotype control condition.



Supplementary Table 1: Clinical and demographic characteristics of patients included in the Nantes cohort used for RT-PCR analysis on colon biopsies.

	Non-IBD controls	Ulcerative Colitis	Crohn Disease
Number	20	21	24
Gender (M/F)	8/12	13/8	9/15
Age (years) (Median, [Min-Max])	47.7 [22.3-67.4]	41.3 [21.4-57.3]	34 [17.4-47.7]
Duration of disease (years) (Median, [Min-Max])	NA ^a	5.7 [0.9-24.7]	9.9 [0.5-27.8]
Endoscopic activity ^b (Y/N)	NA	18/3	19/5
Surgery history (Y/N)		0/21	6/18
Medication ^c (anti-TNF/Immunosuppressor/Corticosteroid)	0/0/0	6/6/3	11/11/0

^a Not Applicable, ^b Activity defined by an endoscopic subscore of MAYO \geq 2

Supplementary Table 2: Clinical and demographic characteristics of UC patients included in the London cohort used for *ex-vivo* organ culture.

ID	Material	Age	Gender	Treatment	Collected	Diagnosed	Location	Inflammation
2122	Biopsy	69	F	Pentasa	2016	2012	colon	+++
2110	Resection	62	F	Aza/Vedolizumab	2016	2013	Sigmoid/ Rectum	+++
2113	Biopsy	32	M	None	2016	2004	Colon	++++
2114	Biopsy	34	M	Methotrexate/Pentasa	2016	2006	Colon	++
2117	Biopsy	39	M	Methotrexate/Pentasa/ prednisolone	2016	2008	colon	++
2126	Biopsy	30	M	None	2016	2015	Colon	++
2245	Resection	61	M	None	2016	N.D.	Colon	+++
2264	Biopsy	56	F	SPZ/Sulfasalazine	2016	N.D.	Colon	+++
2289	Resection	36	M	None	2016	2011	Rectum	+
2291	Resection	49	F	none	2016	2000	Rectum	+++

Supplementary Methods:

Datasets and cohort characteristic

For cohort GSE38713 (40), non-IBD controls (n=13) underwent a colonoscopy for mild gastrointestinal symptoms or a screening for CRC. Biopsies were always also taken in unaffected sigmoid or rectum. Inclusion criteria for patients with UC were age between 18 and 65, a diagnosis of UC for at least 6 months before the enrollment and no infection. Active disease was defined by a total MAYO ≥ 4 with at least 1 point in the bleeding sub-score and an endoscopic sub-score ≥ 2 . Inactive disease was defined by a total MAYO score < 4 with an endoscopic sub-score of 0. All inactive patients were in remission for at least 5 months before enrollment. Uninvolved mucosa has been defined by a normal endoscopic appearance more a normal histology and the absence of previous disease activity. Non-IBD controls have been compared to 15 patients with UC during an active phase and 8 patients with UC in remission. There was no significant difference concerning demographic and clinical parameters. None of the patients were treated by anti-TNFs.

Cohort GSE59071 (41) included 11 non-IBD patients (controls), 97 patients with UC and 8 with CD. Non-IBD controls underwent a colonoscopy for a screening for CRC. All biopsies were taken in unaffected colon or rectum in controls and in the most inflamed part of the colon in patients with IBD. Disease activity was endoscopically assessed. In UC, 74 patients with active disease (endoscopic sub-score of 2-3) and 23 with inactive disease (endoscopic sub-score of 0-1) were included. All the patients with CD (n=8) had active disease assessed by the presence of ulcerations.

Cohort GSE57945 (42) enrolled children and adolescents younger than 17 years who underwent ileo-colonoscopy for suspected IBD or non-specific GI symptoms. Only patients with a

confirmed persisting diagnosis of CD, UC or non-IBD controls during an average of 22 months' follow-up were included in the cohort. Age-matched patients with CD, UC and non-IBD controls were analyzed. Colonic or ileal location of the disease has to be proven histologically. Patients with CD were divided into two groups depending on the location of the lesions: pure colonic disease (L3) and ileal and/or ileo-colonic disease (L1 or L3).

Cohort GSE16879 (43) enrolled patients with active IBD despite corticosteroids and/or immunosuppressant (24 UC, 19 colonic CD, 18 ileal CD). Twelve non-IBD patients who underwent ileo-colonoscopy for CRC screening served as controls. Biopsies were taken into the colon (n=6) and into the ileum (n=6) in non-IBD controls. For IBD patients, biopsies were taken during colonoscopies performed within a week before the first infusion of infliximab (5 mg/Kg) into the colon (UC and colonic CD) or the ileum (ileal CD). A second endoscopy with biopsies was performed at week 4 for the patient who received only one infusion at week 0 and, at week 6 for the patients who received a loading dose at week 0, 2 and 6. For colonic CD, the response was defined as a complete mucosal healing and a decrease of at least 3 points of the histological score for CD (47). For UC, the response was defined as a complete mucosal healing (MAYO endoscopic sub-score of 0-1) with a grade 0 or 1 on the histologic score (Geboes). For patients with an ileal CD, the response was defined by a clear improvement of the ulcerations and a decrease on the histological score. On the 43 patients with colonic IBD, 20 were responders (8 UC and 12 CD) and of the 18 ileal CD, 8 were responders.

Cohort GSE12251 (44) has enrolled 22 patients with an active disease despite corticosteroids and/or immunosuppressant initially included in the ACT-1 phase III study of infliximab. The disease activity was defined by a total MAYO score between 6 and 12 and a MAYO endoscopic sub-score ≥ 2 . All the patients were treated by infliximab 5 or 10 mg/Kg at week 0, 2 and 6.

Biopsies were collected before the first infusion of infliximab and at week 8 into the sigmoid (15 to 20 cm from the anal verge). Response, assessed 8 weeks after the first infusion of infliximab, was defined by an endoscopic sub-score of 0-1 and a grade 0 or 1 on the histological score for UC (Geboes score).

Patients enrolled in cohort GSE23597 (45) participated in an ancillary sub-study of the ACT-1 study. All the patients have a UC in a moderately-to-severely active phase defined by a total MAYO score of 6 to 12. Patients were randomized to receive placebo or infliximab 5mg/Kg (n=15) or 10 mg/Kg (n=17) at week 0,2 and 6 and then every 8 weeks through week 46. Response was defined by a decrease from baseline of the total MAYO score of at least three points and 30% with an accompanying decrease of the bleeding sub-score of at least one point and an absolute bleeding sub-score of 0 or 1. Biopsies were obtained in a subgroup of randomized patients at week 0, 8 and 30 into the sigmoid (15 to 20 cm from the anal verge). There was no difference concerning the concomitant treatment received by the patients at baseline.

Dataset GSE73661 (46) is composed of 2 cohorts treated with vedolizumab or infliximab. Endoscopic-derived biopsies were collected from patients with UC during two phase III trials of vedolizumab, GEMINI I and GEMINI LTS. GEMINI I was a phase III randomized, placebo-controlled, double-blinded, multicenter study investigating induction and maintenance of clinical response and remission by vedolizumab in patients with moderate-to-severe UC, and GEMINI LTS is an ongoing multicentre, open-label study on long-term safety and efficacy of vedolizumab in patients with UC and CD. Altogether 41 patients (31 patients from GEMINI I and 13 from GEMINI LTS) treated with vedolizumab at inclusion were included. Biopsies were taken at protocol-specified time points (W0, W6, W12 and W52, or at study withdrawal). As

control groups, colonic mucosal biopsies were collected from 23 patients with UC before and W4–6 after first IFX therapy as well as from 12 non-IBD control individuals with normal mucosa. Biopsies were taken in the colon at the edge of ulcers whenever present. If no ulcers were seen, then biopsies were taken at the most inflamed colon segment. H&E stained slides from the paraffin blocks of each patient were scored blindly for features of chronic intestinal inflammation using the histological scoring system of Geboes (S2). Histological mucosal healing was defined as a grade 0 or 1 on the Geboes score and endoscopic mucosal healing was defined as a Mayo endoscopic subscore of 0 or 1.

Human colon RT-qPCR analysis

In addition to the publically available datasets, we analyzed mRNA expression of the IL7R pathway genes in colon biopsies from an unpublished local cohort. Human colon tissues from Crohn's disease and ulcerative colitis patients were collected during endoscopy or during routine surgery at the Nantes University Hospital (Nantes, France) with appropriate ethical approval from the local ethics committee with informed written consent given by the patient. Non-IBD control group tissues for analysis were resected from bowels of patients with colon cancer with samples taken distant from the tumor. All donors were informed of the final use of their samples and signed an informed consent. Total RNA was isolated from macroscopically inflamed and non-inflamed intestinal biopsies of IBD and non-IBD patients using the NucleoSpin RNA Kit (Macherey-Nagel EURL, Hoerdt, France). Reverse transcription was performed using Superscript III Reverse Transcriptase (Invitrogen, Courtaboeuf, France). qRT-PCR was performed in a volume of 15 μ l composed of 1.25 μ l forward and reverse gene-specific primers, 7.5 μ l of Fast Sybr (Invitrogen) and 5 μ l mRNA of the sample at a concentration of 8 or 0.8ng/ μ l RNA equivalent. Amplification conditions were optimized for the StepOnePlus real-time PCR systems (Invitrogen). Samples were tested in duplicate and the average values were used for quantification using the $2^{-\Delta\Delta CT}$ method. The following Forward / Reverse

oligonucleotides were used: IL7: TGACTTGTGTTTCCTAAAGAGACT/
GGAGGATGCAGCTAAAGTTCG, IL7 full: TGAGAGTGTTCTAATGGTCAGCA/
TGGTTTTCTTCCTTTAACCTGGC, IL7R α all: AGGGAGAGTGGCAAGAATGG/
TTGTCGCTCACGGTAAGTTCA, IL7R α mb: TTGGTCATCTTGGCCTGTGT/
CACCTATGAATCTGGCAGTC, gamma-chain: CCACTGTTTGGAGCACTTGG/
TTGGGTGGCTCCATTCCTC, TSLP: CCACTGTTTGGAGCACTTGG/
TTGGGTGGCTCCATTCCTC, TSLPR: CAGAGCAGCGAGACGACATT/
GGACAGGTCAGAACACGTCA, TNF: CCCGAGTGACAAGCCTGTAG/
TGAGGTACAGGCCCTCTGAT, TNFR1: C TTCAGAAGTGGGAGGACAGC/
TCGATCTCGTGGTCGCTCAG, TNFR2: CCAGTGCGTTGGACAGAAG/
GCTGCTACAGACGTTACGA, ITGA4: TCAATCCCGGGGCGATTTAC/
TGAAAGTGTGACCCCAAC, ITGB7: TAAGTCTGCAGTTGGGGAGC/
AGAGTGTTCAAGGGTCACGG.

Preparation of Human Lamina Propria Single Cell Suspension

Biopsies were collected in ice cold RPMI 1640 (Corning Inc., Corning, NY) and processed within 30 min following colonoscopy. Epithelial layer dissociation was performed with 2 cycles of incubation in EDTA-enriched dissociation medium (HBSS w/o Ca²⁺ Mg²⁺ (Life Technologies, Carlsbad, CA) - HEPES 10mM (Life Technologies) - EDTA 5mM (Life Technologies)) for 15 minutes at +37°C under 100 rpm agitation. Biopsies were then washed in complete RPMI media and transferred in digestion medium (HBSS with Ca²⁺ Mg²⁺ - FCS 2% - DNase I 0.5mg/ml (Sigma-Aldrich, St. Louis, MO) – Collagenase IV 0.5mg/ml (Sigma-Aldrich)) for 40 minutes at +37°C under 100 rpm agitation. The cell suspension was then filtered through a 70 μ m cell strainer and washed. After red blood cell lysis (BioLegend, San Diego, CA) and washing, dead cells were depleted from the suspension using the dead cell

depletion kit (Miltenyi Biotec, Bergisch Gladbach, Germany), following manufacturer's recommendations. Viability of the final cell suspension was calculated using a hemocytometer and Trypan blue (Corning) exclusion and was > 85%.

CyTOF analyses

Tissue cell suspensions were first incubated with Rh103 intercalator (Fluidigm, San Francisco, CA) for 20 minutes at 37°C to label non-viable cells, and then washed and labeled with a panel of metal-labeled antibodies for 30 mins on ice. The samples were then fixed and permeabilized with BD Cytotfix/Cytoperm (BD Biosciences) and incubated in 0.125nM Ir intercalator (Fluidigm) diluted in PBS containing 2% formaldehyde for 30 mins. The samples were then washed and stored in PBS containing 0.2% BSA at 4°C until acquisition. Immediately prior to acquisition, samples were washed once with PBS, once with de-ionized water and then resuspended at a concentration of 1 million cells/ml in deionized water containing a 1:20 dilution of EQ 4 Element Beads (Fluidigm). The samples were acquired on a CyTOF2 (Fluidigm) equipped with a SuperSampler fluidics system (Victorian Airships) at an event rate of <500 events/second. FCS files were manually pre-gated on Ir193 DNA+ events, excluding dead cells, doublets, and DNA- negative debris. The samples were analyzed using a combination of manual gating based on the expression of canonical markers and dimensionality reducing data visualization using viSNE (93) based on all phenotypic markers. Putative cell populations on the resulting viSNE maps were manually gated based on the expression of canonical markers. Statistics for defined cell populations were exported and analyzed using Prism (Graphpad Software).

Flow cytometry

The following monoclonal antibodies (mAbs) were used for flow cytometry experiments: anti-mouse CD45 (30-F11), anti-mouse ITGA4 (9F10) and anti-human CD45 (HI30), CD3 (UCHT-1), CD4 (L200), CD25 (M-A251), CD127 (hIL7R-M21), CCR6 (11A9), CCR9 (112509), CCR5 (2D7), CXCR3 (1C6), ITGA4 (9F10), ITGAE (Ber-ACT8), MADCAM1 (314G8), pSTAT5 (47/stat5 pY694) were purchased from BD Biosciences. Fluorescent mAbs anti-human CD127 (eBioRDR5), anti-human/mouse ITGB7 (FIB504), anti-human ITGB1 (TS2/16) were purchased from ebioscience. Fluorescent mAbs anti-human GPR15 (clone # 367902) and recombinant protein mouse and human MADCAM1 were purchased from R&D Systems. Fluorescent mAbs anti-human ITGA4-ITGB7 (Act-1) were donated by the NIH AIDS Research & Reference Reagent program. Flow cytometry analysis was performed using a BD LSRII flow cytometer (BD Bioscience) and FlowJo software. Cell subpopulations were purified using an ARIA II flow cytometer (BD Bioscience).

Cell culture and analysis of $\alpha 4\beta 7$ expression

Human PBMC were extracted from the blood of healthy donors (EFS, Nantes) by Ficoll gradient centrifugation (GE Healthcare Life Science, Paris, France). Red blood cells were lysed and the cells washed before reconstitution in serum-free TexMacs medium (Miltenyi Biotec). C57Bl/6 mouse PBMC and splenocytes were isolated using a similar procedure and then cultured in RPMI 1640 medium (Thermofisher) supplemented with 2mM L-glutamine, 100 U/ml penicillin, 0.1mg/ml streptomycin, 1% non-essential amino acids, 10mM HEPES, 1mM sodium pyruvate, and 50 μ M 2-Mercaptoethanol. T cells were isolated using untouched CD3+ Tcell Kit (Miltenyi). T-cell subpopulations (CD4+CD25+CD127^{low} and CD4+CD25-CD127^{high}) were sorted using a non-antagonistic antibody against CD127 from ebioscience (eBioRDR5) and an ARIA II cell sorter. Recombinant human or mouse IL7 (BioRad) were added at the doses indicated in each experiment with cells cultured at 37°C and 5% CO₂ in

p96-U bottom plate or F25 Flask (BD-Falcon). In some conditions, a dose-response of anti-IL7R α mAb (clone N13B2, Ose Immunotherapeutics, France) was added before addition of IL7. The surface expression of integrin or chemokine receptor proteins were analyzed at different time-points by flow cytometry, and in some conditions after cell permeabilization or with MnCl₂ buffer (Sigma Aldrich) to allow conformational change of integrin. In some conditions, T cells were pre-treated with different inhibitors of protein transcription (Actinomycin D), protein synthesis (Cycloheximide) and protein transport (Brefeldin A or Monensin A), or signaling inhibitor molecules such as Ruxolitinib (inhibitor of Jak1/Jak2) (Sigma Aldrich), Jak 3 Inhibitor (Merck Millipore), STAT 5 inhibitor (Merck Millipore), Wortmanine (inhibitor of PI3K) (Merck Millipore), LY294002 (inhibitor of PI3K) (Sigma Aldrich), CREB-CBP inhibitor (CAS 92-78-4-Calbiochem) and CBP-P300 histone acetyltransferase inhibitor (CAS 328968-36-1-Calbiochem).

Supplemental references:

S1. Peck BC, et al. MicroRNAs classify different disease behavior phenotypes of Crohn's disease and may have prognostic utility. *Inflamm Bowel Dis*. 2015;21(9):2178–2187.

S2. Geboes K, et al. A reproducible grading scale for histological assessment of inflammation in ulcerative colitis. *Gut*. 2000;47(3):404–409.